

Boundary Operator Product Expansion Coefficients of the Three-dimensional Ising Universality Class

Dorian Przetakiewicz,^{✉,*} Stefan Wessel,^{✉,†} and Francesco Parisen Toldin^{✉,‡}

Institute for Theoretical Solid State Physics, RWTH Aachen University, Otto-Blumenthal-Str. 26, 52074 Aachen, Germany

Recent advances in field theory and critical phenomena have focused on the characterization of boundary or defects in a conformally-invariant system. In this Letter we study the critical behavior of the three-dimensional Ising universality class in the presence of a surface, realizing the ordinary, the special, and the normal universality classes. By using high-precision Monte Carlo simulations of an improved model, where leading scaling corrections are suppressed, and a finite-size scaling analysis, we determine unbiased, accurate estimates of universal boundary operator product expansion coefficients. Furthermore, we improve the value of the scaling dimension of the surface field at the special transition by the estimate $\hat{\Delta}_\sigma = 0.3531(3)$.

Introduction.— The modern theory of critical phenomena is a cornerstone of contemporary physics, bridging key concepts from fundamental physics, statistical mechanics, and condensed matter physics. A central focus is the characterization of universal quantities — properties that assume specific values within a given universality class (UC), regardless of the underlying microscopic details of a system. Well-known examples include critical exponents, amplitude ratios, and coefficients in operator product expansions (OPE). The latter in fact encode the renormalization group (RG) flow near fixed points, and are fundamental ingredients in the characterization of conformal invariance at a critical point [1]. In many realistic scenarios, it is necessary to extend beyond the standard field-theoretical and RG approaches to bulk criticality and consider the effects of boundaries, such as those encountered in surface critical phenomena [2]. Recent years have seen significant advances in our understanding of critical many-body systems with boundaries, such as classical [3–8] and quantum magnets [9–21], and gapless quantum systems with topologically-protected boundary states [22–34]. While the overall phase diagrams of many such systems have been well-characterized through field-theoretical and computational analyses, new and unexpected RG fixed points, such as the extraordinary log surface transition, have recently been predicted [35] and explored both within the RG and numerically [3–6, 8, 17, 36]. Simultaneously, conformal field theory (CFT) has provided insights into various universal properties, such as boundary OPE (BOPE) coefficients, for critical three-dimensional systems with surfaces. Using advanced approximate techniques, such the truncated conformal bootstrap (TCB) [37] and the fuzzy sphere (FZ) construction [38], some of these OPE coefficients have been estimated recently [39, 40]. However, unbiased estimates for these universal numbers often still remain unknown, even for the fundamental UC of the three-dimensional Ising model, which corresponds to scalar ϕ^4 theory. In this case, different characteristic surface UCs emerge, depending on the surface enhancement of interactions. For surface interactions preserving the \mathbb{Z}_2 -symmetry, the ordinary UC and the extraordinary UC arise for weak and strong surface enhancement, respectively, with the special UC separating them. A finite surface-ordering field explicitly breaking the \mathbb{Z}_2 -symmetry realizes the normal UC, equiva-

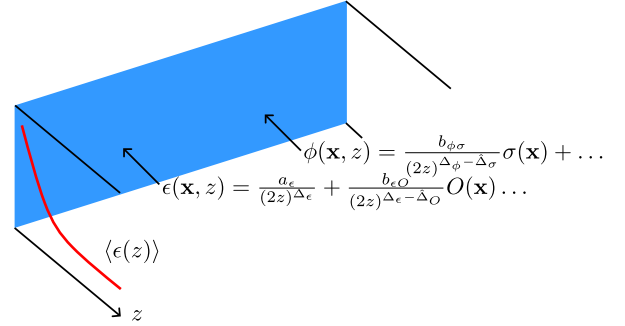


FIG. 1. Illustration of the BOPE.

lent to the extraordinary UC [41]. The presence of a surface restricts the conformal symmetry to the subgroup of transformations that leave the boundary invariant [42]. Accordingly, one distinguishes between *bulk* and *surface* operators, the latter admitting a usual OPE. Close to the surface, bulk operators admit a BOPE [43, 44], whose form is fixed by CFT. Here, we bridge the gap between such a general structure and the actual universal values by using accurate and unbiased Monte Carlo (MC) simulations in order to extract the universal coefficients of these OPEs for the 3D Ising surface UCs.

The spectrum of the bulk Ising UC contains two relevant operators: the \mathbb{Z}_2 -even energy operator ϵ and the \mathbb{Z}_2 -odd magnetization operator ϕ . Introducing coordinates (\mathbf{x}, z) , where $\mathbf{x}(z)$ is parallel (perpendicular) to the surface, the BOPE for the ordinary and special UC reads [44]

$$\phi(\mathbf{x}, z) \underset{z \rightarrow 0}{=} \frac{b_{\phi\sigma}}{(2z)^{\Delta_\phi - \Delta_\sigma}} \sigma(\mathbf{x}) + \dots, \quad (1)$$

$$\epsilon(\mathbf{x}, z) \underset{z \rightarrow 0}{=} \frac{a_\epsilon}{(2z)^{\Delta_\epsilon}} + \frac{b_{\epsilon O}}{(2z)^{\Delta_\epsilon - \Delta_O}} O(\mathbf{x}) \dots \quad (2)$$

Here, σ is the lowest-lying \mathbb{Z}_2 -odd surface operator, associated with the surface magnetization, with dimension $\hat{\Delta}_\sigma$, while O is the lowest-lying \mathbb{Z}_2 -even surface operator with dimension $\hat{\Delta}_O$. The BOPE is illustrated in Fig. 1. In addition, by fusing $\sigma(\mathbf{0})$ with $\phi(\mathbf{0}, z)$ one obtains [5]:

$$\sigma(\mathbf{0})\phi(\mathbf{0}, z) \underset{z \rightarrow 0}{=} b_{\phi\sigma} \frac{2^{\hat{\Delta}_\sigma - \Delta_\phi}}{z^{\hat{\Delta}_\sigma + \Delta_\phi}} \left[1 + \beta_{\phi\sigma O} z^{\hat{\Delta}_O} O(\mathbf{0}) + \dots \right]. \quad (3)$$

TABLE I. Universal BOPE coefficients. The quoted uncertainties for TCB[45] and FZ results are only estimates of their systematic errors.

Ordinary UC						
$b_{\phi\sigma}$	a_ϵ	$b_{\epsilon D}$	$\beta_{\phi\sigma D}$	$\lambda_{\sigma\sigma D}$	C_D	Method and Ref.
0.870(3)	-0.753(3)	-0.84(1)	1.05(3)	1.44(7)	0.0101(3)	MC, this work
0.869(7)	-0.750(3)					TCB [39]
0.87(2)	-0.74(4)	-0.92(4)			0.0089(2)	FZ [40]
Special UC						
$b_{\phi\sigma}$	a_ϵ	$b_{\epsilon\epsilon}$	$\beta_{\phi\sigma\epsilon}$	$\lambda_{\sigma\sigma\epsilon}$	$\lambda_{\epsilon\epsilon\epsilon}$	Method and Ref.
1.435(3)	1.160(4)	3.09(5)	0.79(1)	0.86(1)	1.02(2)	MC, this work
Normal UC						
a_ϕ	$b_{\phi D}$	a_ϵ	$b_{\epsilon D}$	C_D		Method and Ref.
2.6143(5)	0.242(2)	6.679(6)	1.69(1)	0.198(3)		MC, this work
2.60(5)	0.244(8)			0.193(5)		MC [5, 46]
2.599(1)	0.25064(6)	6.607(7)	1.742(6)	0.182(1)		TCB [39]
2.58(16)	0.254(17)	6.4(9)	1.74(22)	0.176(2)		FZ [40]

In Eqs. (1)-(3) a_ϵ , $b_{\epsilon O}$, $b_{\phi\sigma}$ and $\beta_{\phi\sigma O}$ are universal BOPE coefficients. Dots indicate subleading contributions arising from descendants of σ and O , as well as surface operators of higher dimension. In the ordinary UC there are no relevant \mathbb{Z}_2 -even operators, and the leading operator O in Eq. (2) is the displacement operator D , with dimension is $\hat{\Delta}_D = 3$ [47, 48]. In the special UC, the leading operator O is instead the relevant surface \mathbb{Z}_2 -even operator ϵ , associated with the deviation of the enhancement of surface interactions from its critical value.

In the normal UC there are no relevant operators and the lowest surface operator is the displacement D . The \mathbb{Z}_2 -symmetry is broken on the boundary, so that a classification of surface operators in terms of \mathbb{Z}_2 -symmetry does not apply. Accordingly, Eq. (1) is modified as follows:

$$\phi(\mathbf{x}, z) \underset{z \rightarrow 0}{=} \frac{a_\phi}{(2z)^{\Delta_\phi}} + \frac{b_{\phi D}}{(2z)^{\Delta_\phi - 3}} D(\mathbf{x}) + \dots, \quad (4)$$

with a_ϕ and $b_{\phi D}$ universal BOPE coefficients. The BOPE of the energy operator holds as in Eq. (2), with $O = D$.

The various BOPE coefficients — the main target of this work — are summarized in Table I. They are extracted from the 1- and 2-point correlations that follow from Eqs. (1)-(4). In particular, in the ordinary and special UC, we use the surface-bulk 2-point correlator with leading scaling

$$\langle \sigma(\mathbf{0}) \phi(\mathbf{0}, z) \rangle = b_{\phi\sigma} \frac{2^{\hat{\Delta}_\sigma - \Delta_\phi}}{z^{\hat{\Delta}_\sigma + \Delta_\phi}} \left[1 + \beta_{\phi\sigma O} z^{\hat{\Delta}_O} \langle O(\mathbf{0}) \rangle \right], \quad (5)$$

while in the normal UC we exploit the 1-point function with

$$\langle \phi(\mathbf{x}, z) \rangle = \frac{a_\phi}{(2z)^{\Delta_\phi}} + \frac{b_{\phi D}}{(2z)^{\Delta_\phi - 3}} \langle D(\mathbf{x}) \rangle. \quad (6)$$

Further, for all surface UC considered, the 1-point function of the energy operator obeys

$$\langle \epsilon(\mathbf{x}, z) \rangle = \frac{a_\epsilon}{(2z)^{\Delta_\epsilon}} + \frac{b_{\epsilon O}}{(2z)^{\Delta_\epsilon - \hat{\Delta}_O}} \langle O(\mathbf{x}) \rangle. \quad (7)$$

Model.— We simulate the Blume-Capel model [49, 50] on a three-dimensional lattice. Its reduced Hamiltonian is

$$\mathcal{H} = -\beta \sum_{\langle xx' \rangle} S_x S_{x'} + \delta \sum_x S_x^2, \quad S_x = -1, 0, 1, \quad (8)$$

such that the Gibbs weight is $\exp(-\mathcal{H})$. In Eq. (8) the first sum extends over nearest-neighbor sites and the second sum over all lattice sites. In the limit $\delta \rightarrow -\infty$ the Hamiltonian (8) reduces to the Ising model. In the (β, δ) plane, the model exhibits a line of continuous phase transitions in the Ising universality class for $\delta < \delta_{\text{tri}}$, terminating at a tricritical point at $\delta_{\text{tri}} = 2.006(8)$ [51, 52]; see also Refs. [53, 54] for previous determinations of δ_{tri} . For $\delta > \delta_{\text{tri}}$ the model undergoes a first-order phase transition. At $\delta = 0.656(20)$ [55] the Hamiltonian is “improved” [56], i.e., the leading scaling corrections $\propto L^{-\omega}$, with $\omega = 0.832(6)$ [55] are suppressed. As in previous MC studies [46, 57–63], here we fix $\delta = 0.655$ and $\beta = \beta_c = 0.387\,721\,735(25)$ [55], realizing an improved critical model in the Ising UC.

Results.— In order to determine the normalization of bulk fields, we have first simulated the model on a $L \times L \times L$ lattice, with periodic boundary conditions (BCs). We sample the local order parameter S_x and the local energy E_x , defined as

$$E_x \equiv S_x \sum_{\substack{x' \text{ n. n.} \\ \text{of } x}} S_{x'} = S_x \sum_{n=1}^3 (S_{x+e_n} + S_{x-e_n}), \quad (9)$$

where e_n is the unit vector in direction n , so that the sum extends over all nearest neighbor sites of x . The expectation value of E_x and its finite-size amplitude is obtained by fitting $E_{\text{bulk}} \equiv (1/L^3) \sum_x \langle E_x \rangle$ to [64, 65]

$$E_{\text{bulk}} = E_0 + U_E L^{-\Delta_\epsilon}, \quad (10)$$

where $\Delta_\epsilon = 1.412\,625(10)$ [66] is the scaling dimension of the relevant even operator, related to the standard exponent ν by $\Delta_\epsilon = 3 - 1/\nu$ [1]. Fits of MC data [65] allows us to infer estimates of the coefficients E_0 and U_E . In Table II we report

TABLE II. Estimates of the scaling amplitudes as obtained from fits of MC data [65]. For every set of amplitudes we indicate the corresponding UC and the scaling form.

UC	Fit results		Eq.
bulk	$E_0 = 1.204234(8)$	$U_E = 3.496(6)$	(10)
	$\mathcal{N}_S^2 = 0.18566(7)$	$B_{\phi\phi} = 3.386(7)$	(11)
	$\mathcal{N}_E^2 = 1.1790(8)$	$B_{\epsilon\epsilon} = 5.00(8)$	(12)
	$B'_{\epsilon\epsilon} = -9(1)$		
ordinary	$\mathcal{N}_\sigma^2 = 0.383(1)$	$B_{\sigma\sigma} = 4.3(2)$	(15)
	$A_\epsilon = -0.545(2)$	$B_\epsilon = -26.8(8)$	(16)
	$z_0 = 1.01(3)$		
	$M_{\phi\sigma} = 0.392(1)$	$B_{\phi\sigma} = 3.15(9)$	(17)
	$z_0 = 0.99(2)$		
special	$\mathcal{N}_\sigma^2 = 0.3544(6)$	$B_{\sigma\sigma} = 1.49(1)$	(15)
	$A_\epsilon = 0.840(3)$	$B_\epsilon = 5.92(7)$	(16)
	$z_0 = 0.53(2)$		
	$M_{\phi\sigma} = 0.3282(6)$	$B_{\phi\sigma} = 1.38(1)$	(17)
	$z_0 = 0.50(2)$		
	$\mathcal{E}_0 = 1.32291(1)$	$U_\mathcal{E} = 2.12(2)$	(19)
normal (+, o)	$\mathcal{N}_\epsilon^2 = 1.48(2)$	$B_{\epsilon\epsilon} = 1.77(3)$	(20)
	$A_\epsilon = 4.835(4)$	$B_\epsilon = -2.68(8)$	(16)
	$z_0 = 1.43(1)$		
	$A_\phi = 1.12644(6)$	$B_\phi = -1.000(15)$	(21)
	$z_0 = 1.437(3)$		

them, together with other amplitudes discussed below. We fit the two-point function of S_x and E_x to [5, 65]

$$\langle S_x S_0 \rangle = \frac{\mathcal{N}_S^2}{x^{2\Delta_\phi}} \left[1 + B_{\phi\phi} \left(\frac{x}{L} \right)^{\Delta_\epsilon} + Cx^{-2} \right], \quad (11)$$

$$\langle E_x E_0 \rangle_c = \frac{\mathcal{N}_E^2}{x^{2\Delta_\epsilon}} \left[1 + B_{\epsilon\epsilon} \left(\frac{x}{L} \right)^{\Delta_\epsilon} + B'_{\epsilon\epsilon} \left(\frac{x}{L} \right)^{2\Delta_\epsilon} + Cx^{-2} \right], \quad (12)$$

where $\Delta_\phi = 0.5181489(10)$ [66] is the scaling dimension of the relevant odd operator, related to the standard exponent η by $\Delta_\phi = (1 + \eta)/2$ [1] and the subscript c indicates the connected part of the correlations. Eqs. (11) and (12) are valid for $(x/L) \ll 1$ and $x \gtrsim x_0$, with x_0 a nonuniversal length, associated with short-distance behavior. Incidentally, from the results in Table II we can compute the universal finite-size amplitude of the energy operator $u_\epsilon = U_E/\mathcal{N}_E = 3.220(6)$ and the bulk OPE coefficients $\lambda_{\phi\phi\epsilon} = B_{\phi\phi}/u_\epsilon = 1.052(3)$, $\lambda_{\epsilon\epsilon\epsilon} = B_{\epsilon\epsilon}/u_\epsilon = 1.55(2)$, in agreement with MC $\lambda_{\phi\phi\epsilon} = 1.051(1)$, $\lambda_{\epsilon\epsilon\epsilon} = 1.533(5)$ [67], and conformal bootstrap $\lambda_{\phi\phi\epsilon} = 1.0518537(41)$, $\lambda_{\epsilon\epsilon\epsilon} = 1.532435(19)$ [66] estimates.

To realize the various boundary UCs we generalize the Hamiltonian (8), imposing open BCs on one direction, and periodic BC in the remaining two, thus realizing a $L \times L \times L$ lattice with two surfaces S_\downarrow and S_\uparrow , each of size L^2 . The reduced Hamiltonian thus reads

$$\begin{aligned} \mathcal{H} = & -\beta \sum'_{\langle x x' \rangle} S_x S_{x'} + D \sum_x S_x^2 \\ & -\beta_s \sum_{\langle x x' \rangle \in S_\downarrow \cup S_\uparrow} S_x S_{x'} + h_\downarrow \sum_{x \in S_\downarrow} S_x + h_\uparrow \sum_{x \in S_\uparrow} S_x, \end{aligned} \quad (13)$$

where the first sum extends over the nearest-neighbor sites for which at least one site belongs to the bulk, the second over all sites, the third sum over all nearest-neighbor pairs on the boundaries, and the fourth and fifth sums each extend over a single surface. In Eq. (13) we have imposed the same coupling β_s on both surfaces, while we allow for different boundary fields h_\downarrow and h_\uparrow on the two surfaces. The various surface UC studied here are realized by setting the bulk couplings β , D to the improved critical point $D = 0.655$, $\beta = \beta_c = 0.387721735(25)$ [55], and then tuning the boundary parameters β_s , h_\downarrow , h_\uparrow . Due to the reduced translation symmetry, we adopt a slightly different definition for the local energy observable $E_{\mathbf{x},z}$, summing over nearest-neighbor sites along the directions parallel to the surfaces only:

$$E_{\mathbf{x},z} \equiv S_{\mathbf{x},z} \sum_{n=1}^2 (S_{\mathbf{x}+e_n,z} + S_{\mathbf{x}-e_n,z}). \quad (14)$$

We first consider the ordinary UC, which is realized by setting $\beta_s = \beta$ and $h_\downarrow = h_\uparrow = 0$. To extract the normalization of the boundary field, we fit the surface 2-point function to [65]

$$\langle S_{\mathbf{x},0} S_{\mathbf{0},0} \rangle = \frac{\mathcal{N}_\sigma^2}{x^{2\hat{\Delta}_\sigma}} \left[1 + B_{\sigma\sigma} \left(\frac{x}{L} \right)^{\hat{\Delta}} + Cx^{-2} \right], \quad (15)$$

where $\hat{\Delta}_\sigma = 2 - 0.7249(6)$ [58] is the scaling dimension of the lowest odd surface operator σ , and $\hat{\Delta}$ is the dimension of the leading even surface operator appearing in the BOPE $\sigma \times \sigma$, which is the displacement D , with $\hat{\Delta}_D = 3$ [47, 48]. We fit the energy profile to

$$\begin{aligned} \langle E_{\mathbf{x},z} \rangle = & \frac{2}{3} E_0 \\ & + \frac{A_\epsilon}{(2(z+z_0))^{\Delta_\epsilon}} \left[1 + B_\epsilon \left(\frac{z+z_0}{L} \right)^{\hat{\Delta}} + \frac{C}{(z+z_0)^2} \right], \end{aligned} \quad (16)$$

with z_0 a model-dependent correction-to-scaling amplitude [5], $\hat{\Delta} = 3$ and we fix E_0 to the estimate given in Table II; the factor $2/3$ in front of E_0 accounts for the different definitions used in the bulk [Eq. (9)] and with open BCs [Eq. (14)]. The BOPE coefficient $b_{\phi\sigma}$ is extracted from the surface-bulk two-point function, which we fit to

$$\begin{aligned} \langle S_{\mathbf{x},0} S_{\mathbf{x},z} \rangle = & \frac{M_{\phi\sigma}}{(z+z_0)^{\hat{\Delta}_\sigma + \Delta_\phi}} \left[1 + B_{\phi\sigma} \left(\frac{z+z_0}{L} \right)^{\hat{\Delta}} + \frac{C}{(z+z_0)^2} \right], \end{aligned} \quad (17)$$

where $\hat{\Delta}_\sigma = 2 - 0.7249(6)$ [58] is the dimension of the lowest-lying odd surface operator, and as in Eq. (16) $\hat{\Delta} = 3$.

The special UC is realized in the model (13) by setting $\beta_s = 0.54914(2)$ [68]. The analysis of the MC data is analogous to the ordinary UC, with the important difference in the presence of a *relevant* surface \mathbb{Z}_2 -even operator ϵ , so that in Eqs. (15),

(16) and (17) we have $\hat{\Delta} = \hat{\Delta}_\varepsilon = 2 - 0.718(2)$ [68]. In this work we have determined a new estimate of the scaling dimension of the lowest odd operator

$$\hat{\Delta}_\sigma = 0.3531(3), \quad (18)$$

improving an available estimate $\hat{\Delta}_\sigma = 0.3535(6)$ [68]. In fitting the surface-surface and surface-bulk correlations, we use in Eqs. (15) and (17) the value in Eq. (18). For the special UC, we also study the scaling behavior of the surface energy. We fit $E_{\text{surf}} \equiv (1/L^2) \sum_{\mathbf{x}} \langle E_{\mathbf{x},0} \rangle$ to

$$E_{\text{surf}} = \mathcal{E}_0 + U_\varepsilon L^{-\hat{\Delta}_\varepsilon}. \quad (19)$$

Further, to extract the normalization of the surface energy we fit its two-point function to

$$\langle E_{\mathbf{x},0} E_{\mathbf{0},0} \rangle = \frac{\mathcal{N}_\varepsilon^2}{x^{2\hat{\Delta}_\varepsilon}} \left[1 + B_{\varepsilon\varepsilon} \left(\frac{x}{L} \right)^{\hat{\Delta}_\varepsilon} + Cx^{-2} \right]. \quad (20)$$

To realize the normal UC, we set $\beta_s = \beta$ and $h_\downarrow = \infty$ in Eq. (13), thereby polarizing a surface with fixed spins $S = 1$. For the opposite surface, we have considered two cases: a surface with $h_\uparrow = 0$, realizing the ordinary UC, and a surface identical to the lower one, with $h_\uparrow = \infty$. We refer to these BCs as $(+, o)$, and $(+, +)$, respectively. The determination of the BOPE coefficients in the $(+, +)$ BCs delivers results somewhat less precise, though in full agreement with those obtained with $(+, o)$ BCs. Here, we discuss the analysis of the $(+, o)$ case [65]. In the normal UC there are no relevant surface operators, and the lowest-lying operator entering in Eq. (16) is the displacement D , with $\hat{\Delta} = 3$. Furthermore, due to the broken \mathbb{Z}_2 -symmetry, a nonvanishing order-parameter profile emerges in this case, which we fit to

$$\langle S_{\mathbf{x},z} \rangle = \frac{A_\phi}{(2(z+z_0))^{\Delta_\varepsilon}} \left[1 + B_\phi \left(\frac{z+z_0}{L} \right)^3 + \frac{C}{(z+z_0)^2} \right]. \quad (21)$$

Discussion.— As we discuss in App. A, using the fitted amplitudes of Table II one can determine the BOPE coefficients introduced above. In particular, $b_{\phi\sigma} = M_{\phi\sigma} 2^{\Delta_\phi - \hat{\Delta}_\sigma} / (\mathcal{N}_S \mathcal{N}_\sigma)$ [Eq. (16)], $a_\varepsilon = (3/2) A_\varepsilon / \mathcal{N}_E$ [Eq. (17)], and, for the normal UC, $a_\phi = A_\phi / \mathcal{N}_E$ [Eq. (21)]. In the ordinary and normal UC, the finite-size corrections are proportional to the amplitude u_D of the displacement operator D . This enters also in the boundary expansion of the energy-momentum tensor $T_{zz} \underset{z \rightarrow 0}{=} -\sqrt{C_D} D$, where C_D is the universal norm coefficient [69]. On a finite geometry, $\langle T_{zz} \rangle = \Theta / L^3$, where Θ is the universal amplitude of the critical Casimir force [70–77]. The universal norm C_D can be related to the finite-size correction of the 1-point function of the energy and, for the normal UC, of the order parameter [5, 69, 78]

$$C_D = -\frac{2^d \Delta_\varepsilon \Theta}{S_d B_\varepsilon} = -\frac{2 \Delta_\varepsilon \Theta}{\pi B_\varepsilon}, \quad (22)$$

$$C_D = -\frac{2^d \Delta_\phi \Theta}{S_d B_\phi} = -\frac{2 \Delta_\phi \Theta}{\pi B_\phi}, \quad (23)$$

where $S_d = 2\pi^{d/2} / \Gamma(d/2)$ and $d = 3$. Employing the value of Θ reported in App. B, one can determine C_D , as well as the amplitude $u_D = \Theta / \sqrt{C_D}$; for the ordinary UC we obtain $u_D = 3.00(5)$. In the case of the normal UC, Eq. (22) and Eq. (23) provide two different estimators for C_D . In Table I we quote C_D as obtained from Eq. (23), which is more precise, and in full agreement, with that obtained from Eq. (22) $C_D = 0.202(6)$. The finite-size amplitude u_D is found $u_D = 1.34(2)$ [using Eq. (22)] and $u_D = 1.35(1)$ [using Eq. (23)]. The BOPE coefficients $b_{\varepsilon D}$ and $b_{\phi D}$ are extracted from a_ε and a_ϕ with the identities [69]

$$\frac{b_{\varepsilon D}}{\Delta_\varepsilon a_\varepsilon} = \frac{1}{S_d \sqrt{C_D}}, \quad (24)$$

$$\frac{b_{\phi D}}{\Delta_\phi a_\phi} = \frac{1}{S_d \sqrt{C_D}}. \quad (25)$$

Again, in the case of the normal UC, employing on the right-hand side of Eqs. (24)-(25) C_D as extracted from the energy operator [Eq. (22)] gives results in full agreement, though slightly less precise, than those quoted in Table I. Other BOPE coefficients can be extracted as $\beta_{\phi\sigma\varepsilon} = B_{\phi\sigma} / u_D$ and $\lambda_{\sigma\sigma\varepsilon} = B_{\sigma\sigma} / u_D$. In the special UC, finite-size corrections are unrelated to the displacement operator and are due to the lowest-lying \mathbb{Z}_2 -even operator ε . Its finite-size amplitude u_ε can be conveniently obtained from results in Table II as $u_\varepsilon = U_\varepsilon / \mathcal{N}_\varepsilon = 1.74(2)$. Then, BOPE coefficients are obtained as $b_{\varepsilon\varepsilon} = 2^{-\hat{\Delta}_\varepsilon} B_{\varepsilon\varepsilon} a_\varepsilon / u_\varepsilon$, $\beta_{\phi\sigma\varepsilon} = B_{\phi\sigma} / u_\varepsilon$, $\lambda_{\sigma\sigma\varepsilon} = B_{\sigma\sigma} / u_\varepsilon$. The finite-size scaling analysis of the surface energy correlations [Eq. (20)] allows us to extract a further OPE coefficient $\lambda_{\varepsilon\varepsilon\varepsilon} = B_{\varepsilon\varepsilon\varepsilon} / u_\varepsilon$. The remaining BOPE coefficients a_ε and $b_{\phi\sigma}$ are obtained as for the ordinary UC. In Table I we summarize our results, and compare them with available results in the literature. For several quantities we are not aware of previous calculations. Whenever a comparison with previous works is available, we generally observe a reasonable agreement, with a small but significant deviation especially in the estimates of C_D . In the case of the normal UC, our results significantly improve the precision of the universal coefficients obtained in Ref. [5] by reanalyzing some MC results of Ref. [46]. We stress that, different than the TCB and FZ techniques, our method, based on a combination of MC simulations and a finite-size scaling analysis, is numerically exact. As outlined above, and in the SM [65], for some BOPE independent estimates deliver perfectly consistent values, thus underscoring their robustness and the reliability of the quoted uncertainties: we expect our results to provide a benchmark for future studies. Future improvements might be obtained by searching for an improved model where also the leading boundary irrelevant operator, the displacement D , is suppressed. Such a realization, if at all possible, requires however a fine-tuning of surface interactions. The technique used here can be clearly employed for other boundary UCs. In particular, it would be interesting to extend the study to the $O(N)$ model, $N > 1$. While a surface ordinary UC is always present, the special transition exists only for $N \leq N_c$ [35],

with $N_c \approx 5$ [36]. For the $O(N)$ UC, precise estimates of the critical exponents at the ordinary UC are available [7] and the exponents at the special transition have been numerically determined in Refs. [3, 79, 80], whereas a numerically reliable determination of BOPE coefficients is presently not available.

We are grateful to Marco Meineri for useful discussions and comments on the manuscript. We thank Max Metlitski for insightful comments on the manuscript. F.P.T. thanks Martin Hasenbusch for useful communications. F.P.T. is funded by the Deutsche Forschungsgemeinschaft (DFG, German Research Foundation), Project No. 414456783. We gratefully acknowledge the Gauss Centre for Supercomputing e.V. [81] for funding this project by providing computing time through the John von Neumann Institute for Computing (NIC) on the GCS Supercomputer JUWELS at Jülich Supercomputing Centre (JSC). We gratefully acknowledge computing time granted by the IT Center of RWTH Aachen University and used for the calculations of critical Casimir amplitude.

* dorian.przetakiewicz@rwth-aachen.de

† wessel@physik.rwth-aachen.de

‡ parisentoldin@physik.rwth-aachen.de

- [1] J. Cardy, *Scaling and Renormalization in Statistical Physics* (Cambridge University Press, Cambridge, 1996).
- [2] H. W. Diehl, Field-theoretical approach to critical behaviour at surfaces, in *Phase Transitions and Critical Phenomena*, Vol. 10, edited by C. Domb and J. L. Lebowitz (Academic Press, London, 1986) p. 75.
- [3] F. Parisen Toldin, Boundary critical behavior of the three-dimensional Heisenberg universality class, *Phys. Rev. Lett.* **126**, 135701 (2021), arXiv:2012.00039 [cond-mat.stat-mech].
- [4] M. Hu, Y. Deng, and J.-P. Lv, Extraordinary-Log Surface Phase Transition in the Three-Dimensional XY Model, *Phys. Rev. Lett.* **127**, 120603 (2021), arXiv:2104.05152 [cond-mat.stat-mech].
- [5] F. Parisen Toldin and M. A. Metlitski, Boundary criticality of the 3d $O(N)$ model: from normal to extraordinary, *Phys. Rev. Lett.* **128**, 215701 (2022), arXiv:2111.03613 [cond-mat.stat-mech].
- [6] Y. Sun, M. Hu, Y. Deng, and J.-P. Lv, Extraordinary-log Universality of Critical Phenomena in Plane Defects, *Phys. Rev. Lett.* **131**, 207101 (2023), arXiv:2301.11720 [cond-mat.stat-mech].
- [7] F. Parisen Toldin, The ordinary surface universality class of the three-dimensional $O(N)$ model, *Phys. Rev. B* **108**, L020404 (2023), arXiv:2303.16683 [cond-mat.stat-mech].
- [8] F. Parisen Toldin, A. Krishnan, and M. A. Metlitski, Universal finite-size scaling in the extraordinary-log boundary phase of 3d $O(N)$ model, arXiv:2411.05089 [cond-mat.stat-mech].
- [9] L. Zhang and F. Wang, Unconventional Surface Critical Behavior Induced by a Quantum Phase Transition from the Two-Dimensional Affleck-Kennedy-Lieb-Tasaki Phase to a Néel-Ordered Phase, *Phys. Rev. Lett.* **118**, 087201 (2017), arXiv:1611.06477 [cond-mat.str-el].
- [10] C. Ding, L. Zhang, and W. Guo, Engineering Surface Critical Behavior of $(2+1)$ -Dimensional $O(3)$ Quantum Critical Points, *Phys. Rev. Lett.* **120**, 235701 (2018), arXiv:1801.10035 [cond-mat.str-el].
- [11] L. Weber, F. Parisen Toldin, and S. Wessel, Nonordinary edge criticality of two-dimensional quantum critical magnets, *Phys. Rev. B* **98**, 140403(R) (2018), arXiv:1804.06820 [cond-mat.str-el].
- [12] L. Weber and S. Wessel, Nonordinary criticality at the edges of planar spin-1 Heisenberg antiferromagnets, *Phys. Rev. B* **100**, 054437 (2019), arXiv:1906.07051 [cond-mat.str-el].
- [13] L. Weber and S. Wessel, Spin versus bond correlations along dangling edges of quantum critical magnets, *Phys. Rev. B* **103**, L020406 (2021), arXiv:2010.15691 [cond-mat.str-el].
- [14] W. Zhu, C. Ding, L. Zhang, and W. Guo, Surface critical behavior of coupled Haldane chains, *Phys. Rev. B* **103**, 024412 (2021), arXiv:2010.10920 [cond-mat.str-el].
- [15] Y. Xu, C. Peng, Z. Xiong, and L. Zhang, Persistent corner spin mode at the quantum critical point of a plaquette Heisenberg model, *Phys. Rev. B* **106**, 214409 (2022), arXiv:2112.04616 [cond-mat.str-el].
- [16] C. Ding, W. Zhu, W. Guo, and L. Zhang, Special transition and extraordinary phase on the surface of a two-dimensional quantum heisenberg antiferromagnet, *SciPost Physics* **15**, 012 (2023), arXiv:2110.04762 [cond-mat.str-el].
- [17] Y. Sun, J. Lyu, and J.-P. Lv, Classical-quantum correspondence of special and extraordinary-log criticality: Villain's bridge, *Phys. Rev. B* **106**, 174516 (2022), arXiv:2211.11376 [cond-mat.stat-mech].
- [18] Y. Sun and J.-P. Lv, Quantum extraordinary-log universality of boundary critical behavior, *Phys. Rev. B* **106**, 224502 (2022), arXiv:2205.00878 [cond-mat.stat-mech].
- [19] Z. Wang, F. Zhang, and W. Guo, Bulk and surface critical behavior of a quantum Heisenberg antiferromagnet on two-dimensional coupled diagonal ladders, *Phys. Rev. B* **106**, 134407 (2022), arXiv:2207.05248 [cond-mat.str-el].
- [20] X.-J. Yu, R.-Z. Huang, H.-H. Song, L. Xu, C. Ding, and L. Zhang, Conformal Boundary Conditions of Symmetry-Enriched Quantum Critical Spin Chains, *Phys. Rev. Lett.* **129**, 210601 (2022), arXiv:2111.10945 [cond-mat.str-el].
- [21] Y. Liu, H. Shimizu, A. Ueda, and M. Oshikawa, Finite-size corrections to the energy spectra of gapless one-dimensional systems in the presence of boundaries, *SciPost Physics* **17**, 099 (2024), arXiv:2405.06891 [cond-mat.str-el].
- [22] T. Grover and A. Vishwanath, Quantum Criticality in Topological Insulators and Superconductors: Emergence of Strongly Coupled Majoranas and Supersymmetry, arXiv:1206.1332 [cond-mat.str-el].
- [23] M. Barkeshli and X.-L. Qi, Synthetic Topological Qubits in Conventional Bilayer Quantum Hall Systems, *Phys. Rev. X* **4**, 041035 (2014), arXiv:1302.2673 [cond-mat.mes-hall].
- [24] M. Barkeshli, M. Mulligan, and M. P. A. Fisher, Particle-hole symmetry and the composite Fermi liquid, *Phys. Rev. B* **92**, 165125 (2015), arXiv:1502.05404 [cond-mat.str-el].
- [25] J. Cano, M. Cheng, M. Barkeshli, D. J. Clarke, and C. Nayak, Chirality-protected Majorana zero modes at the gapless edge of Abelian quantum Hall states, *Phys. Rev. B* **92**, 195152 (2015), arXiv:1505.07825 [cond-mat.str-el].
- [26] T. Scaffidi, D. E. Parker, and R. Vasseur, Gapless Symmetry-Protected Topological Order, *Phys. Rev. X* **7**, 041048 (2017), arXiv:1705.01557 [cond-mat.str-el].
- [27] D. E. Parker, T. Scaffidi, and R. Vasseur, Topological luttinger liquids from decorated domain walls, *Phys. Rev. B* **97**, 165114 (2018), arXiv:1711.09106 [cond-mat.str-el].
- [28] C.-M. Jian, Y. Xu, X.-C. Wu, and C. Xu, Continuous Néel-VBS quantum phase transition in non-local one-dimensional systems with $SO(3)$ symmetry, *SciPost Phys.* **10**, 033 (2021), arXiv:2004.07852 [cond-mat.str-el].
- [29] R. Thorngren, A. Vishwanath, and R. Verresen, Intrinsically

- gapless topological phases, *Phys. Rev. B* **104**, 075132 (2021), arXiv:2008.06638 [cond-mat.str-el].
- [30] R. Verresen, Topology and edge states survive quantum criticality between topological insulators, arXiv:2003.05453 [cond-mat.str-el].
- [31] R. Verresen, R. Thorngren, N. G. Jones, and F. Pollmann, Gapless Topological Phases and Symmetry-Enriched Quantum Criticality, *Phys. Rev. X* **11**, 041059 (2021), arXiv:1905.06969 [cond-mat.str-el].
- [32] R. Wen and A. C. Potter, Bulk-boundary correspondence for intrinsically gapless symmetry-protected topological phases from group cohomology, *Phys. Rev. B* **107**, 245127 (2023), arXiv:2208.09001 [cond-mat.str-el].
- [33] R. Wen and A. C. Potter, Classification of 1+1d gapless symmetry protected phases via topological holography, arXiv:2311.00050 [cond-mat.str-el].
- [34] N. Myerson-Jain, X.-C. Wu, and C. Xu, Pristine and Pseudogapped Boundaries of the Deconfined Quantum Critical Points, arXiv:2405.18481 [cond-mat.str-el].
- [35] M. A. Metlitski, Boundary criticality of the $O(N)$ model in $d = 3$ critically revisited, *SciPost Phys.* **12**, 131 (2022), arXiv:2009.05119 [cond-mat.str-el].
- [36] J. Padayasi, A. Krishnan, M. A. Metlitski, I. A. Gruzberg, and M. Meineri, The extraordinary boundary transition in the 3d $O(N)$ model via conformal bootstrap, *SciPost Physics* **12**, 190 (2022), arXiv:2111.03071 [cond-mat.stat-mech].
- [37] F. Gliozzi, Constraints on Conformal Field Theories in Diverse Dimensions from the Bootstrap Mechanism, *Phys. Rev. Lett.* **111**, 161602 (2013), arXiv:1307.3111 [hep-th].
- [38] W. Zhu, C. Han, E. Huffman, J. S. Hofmann, and Y.-C. He, Uncovering Conformal Symmetry in the 3D Ising Transition: State-Operator Correspondence from a Quantum Fuzzy Sphere Regularization, *Phys. Rev. X* **13**, 021009 (2023), arXiv:2210.13482 [cond-mat.stat-mech].
- [39] F. Gliozzi, P. Liendo, M. Meineri, and A. Rago, Boundary and interface CFTs from the conformal bootstrap, *J. High Energy Phys.* **2015**, 36, arXiv:1502.07217 [hep-th].
- [40] Z. Zhou and Y. Zou, Studying the 3d Ising surface CFTs on the fuzzy sphere, *SciPost Physics* **18**, 031 (2025), arXiv:2407.15914 [hep-th].
- [41] H. W. Diehl, Critical adsorption of fluids and the equivalence of extraordinary to normal surface transitions, *Ber. Bunsenges. Phys. Chem.* **98**, 466 (1994).
- [42] J. L. Cardy, Conformal invariance and surface critical behavior, *Nucl. Phys. B* **240**, 514 (1984).
- [43] H. W. Diehl and S. Dietrich, Field-theoretical approach to static critical phenomena in semi-infinite systems, *Z. Phys. B* **42**, 65 (1981); Erratum: Field-theoretical approach to static critical phenomena in semi-infinite systems, *Z. Phys. B* **43**, 281 (1981).
- [44] D. M. McAvity and H. Osborn, Conformal field theories near a boundary in general dimensions, *Nucl. Phys. B* **455**, 522 (1995), arXiv:cond-mat/9505127 [cond-mat].
- [45] In order to extract a_ϵ in the ordinary UC from the results of Ref. [39] we have employed the Conformal Bootstrap determination of the bulk OPE coefficients of [66]. The quoted value of C_D is extracted from x_ϵ in Eq. (3.17) of Ref. [39]; with our normalization $C_D = (x_\epsilon/(4\pi))^2$. Using x_σ in Eq. (3.17) of Ref. [39] one obtains a similar value $C_D = 0.1828(2)$.
- [46] F. Parisen Toldin and S. Dietrich, Critical Casimir forces and adsorption profiles in the presence of a chemically structured substrate, *J. Stat. Mech.: Theory Exp.* **P11003**, , arXiv:1007.3913 [cond-mat.stat-mech].
- [47] T. W. Burkhardt and J. L. Cardy, Surface critical behaviour and local operators with boundary-induced critical profiles, *J. Phys. A: Math. Gen.* **20**, L233 (1987).
- [48] M. Billò, V. Gonçalves, E. Lauria, and M. Meineri, Defects in conformal field theory, *J. High Energy Phys.* **2016** (4), 91, arXiv:1601.02883 [hep-th].
- [49] M. Blume, Theory of the First-Order Magnetic Phase Change in UO_2 , *Phys. Rev.* **141**, 517 (1966).
- [50] H. W. Capel, On the possibility of first-order phase transitions in Ising systems of triplet ions with zero-field splitting, *Physica* **32**, 966 (1966).
- [51] M. Deserno, Tricriticality and the Blume-Capel model: A Monte Carlo study within the microcanonical ensemble, *Phys. Rev. E* **56**, 5204 (1997).
- [52] J. Zierenberg, N. G. Fytas, and W. Janke, Parallel multicanonical study of the three-dimensional Blume-Capel model, *Phys. Rev. E* **91**, 032126 (2015), arXiv:1502.07214 [cond-mat.stat-mech].
- [53] J. R. Heringa and H. W. J. Blöte, Geometric cluster Monte Carlo simulation, *Phys. Rev. E* **57**, 4976 (1998).
- [54] Y. Deng and H. W. J. Blöte, Constrained tricritical Blume-Capel model in three dimensions, *Phys. Rev. E* **70**, 046111 (2004).
- [55] M. Hasenbusch, Finite size scaling study of lattice models in the three-dimensional Ising universality class, *Phys. Rev. B* **82**, 174433 (2010), arXiv:1004.4486 [cond-mat.stat-mech].
- [56] A. Pelissetto and E. Vicari, Critical phenomena and renormalization-group theory, *Phys. Rep.* **368**, 549 (2002), arXiv:cond-mat/0012164.
- [57] M. Hasenbusch, Thermodynamic Casimir effect for films in the three-dimensional Ising universality class: Symmetry-breaking boundary conditions, *Phys. Rev. B* **82**, 104425 (2010), arXiv:1005.4749 [cond-mat.stat-mech].
- [58] M. Hasenbusch, Thermodynamic Casimir force: A Monte Carlo study of the crossover between the ordinary and the normal surface universality class, *Phys. Rev. B* **83**, 134425 (2011), arXiv:1012.4986 [cond-mat.stat-mech].
- [59] F. Parisen Toldin, M. Tröndle, and S. Dietrich, Critical Casimir forces between homogeneous and chemically striped surfaces, *Phys. Rev. E* **88**, 052110 (2013), arXiv:1303.6104 [cond-mat.stat-mech].
- [60] F. Parisen Toldin, M. Tröndle, and S. Dietrich, Line contribution to the critical Casimir force between a homogeneous and a chemically stepped surface, *J. Phys.: Condens. Matter* **27**, 214010 (2015), arXiv:1409.5536 [cond-mat.stat-mech].
- [61] M. Hasenbusch, Thermodynamic Casimir Effect in Films: the Exchange Cluster Algorithm, *Phys. Rev. E* **91**, 022110 (2015), arXiv:1410.7161 [cond-mat.stat-mech].
- [62] F. Parisen Toldin, Critical Casimir force in the presence of random local adsorption preference, *Phys. Rev. E* **91**, 032105 (2015), arXiv:1308.5220 [cond-mat.stat-mech].
- [63] F. Parisen Toldin, F. F. Assaad, and S. Wessel, Critical behavior in the presence of an order-parameter pinning field, *Phys. Rev. B* **95**, 014401 (2017), arXiv:1607.04270 [cond-mat.stat-mech].
- [64] A. P. Young, *Everything You Wanted to Know About Data Analysis and Fitting but Were Afraid to Ask*, Springer-Briefs in Physics (Springer International Publishing, 2015) arXiv:1210.3781.
- [65] See Supplemental Material for a discussion of the scaling forms of model observables, results of the fits of MC data, and some additional results.
- [66] F. Kos, D. Poland, D. Simmons-Duffin, and A. Vichi, Precision islands in the Ising and $O(N)$ models, *J. High Energy Phys.* **2016** (8), 36, arXiv:1603.04436 [hep-th].
- [67] M. Hasenbusch, Two- and three-point functions at criticality: Monte Carlo simulations of the improved three-dimensional Blume-Capel model, *Phys. Rev. E* **97**, 012119

- (2018), arXiv:1711.10946 [hep-lat].
- [68] M. Hasenbusch, Monte Carlo study of surface critical phenomena: The special point, *Phys. Rev. B* **84**, 134405 (2011), arXiv:1108.2425 [cond-mat.stat-mech].
- [69] J. L. Cardy, Universal critical-point amplitudes in parallel-plate geometries, *Phys. Rev. Lett.* **65**, 1443 (1990).
- [70] M. E. Fisher and P.-G. de Gennes, Phénomènes aux parois dans un mélange binaire critique, *C. R. Acad. Sci. Paris Ser. B* **287**, 207 (1978).
- [71] M. Krech, *The Casimir Effect in Critical Systems* (World Scientific, London, 1994).
- [72] M. Krech, Fluctuation-induced forces in critical fluids, *J. Phys.: Condens. Matter* **11**, R391 (1999), arXiv:cond-mat/9909413.
- [73] J. G. Brankov, D. M. Danchev, and N. S. Tonchev, *Theory of Critical Phenomena in Finite-size Systems: Scaling and Quantum Effects*, Series in modern condensed matter physics (World Scientific, Singapore, 2000).
- [74] A. Gambassi, The Casimir effect: From quantum to critical fluctuations, *J. Phys.: Conf. Ser.* **161**, 012037 (2009), arXiv:0812.0935 [cond-mat.stat-mech].
- [75] A. Gambassi and S. Dietrich, Critical Casimir forces steered by patterned substrates, *Soft Matter* **7**, 1247 (2011), arXiv:1011.1831 [cond-mat.soft].
- [76] A. Maciołek and S. Dietrich, Collective behavior of colloids due to critical Casimir interactions, *Rev. Mod. Phys.* **90**, 045001 (2018), arXiv:1712.06678 [cond-mat.soft].
- [77] D. M. Dantchev and S. Dietrich, Critical Casimir effect: Exact results, *Phys. Rep.* **1005**, 1 (2023), arXiv:2203.15050 [cond-mat.stat-mech].
- [78] We adopt the normalization of the energy-momentum tensor used in Ref. [5], which differs from that of Ref. [69]. In our convention, $\langle T_{zz} \rangle$ equals the critical Casimir force Θ/L^3 (See also App. B). Compared to Ref. [69], our definition of the energy-momentum tensor incorporates a factor $-S_d^{-1}$, and the universal coefficient c of Eq. (1) in Ref. [69] is related to the universal norm C_D by $C_D = 4(d-1)/(S_d^2 d)c$.
- [79] Y. Deng, H. W. J. Blöte, and M. P. Nightingale, Surface and bulk transitions in three-dimensional O(n) models, *Phys. Rev. E* **72**, 016128 (2005), arXiv:cond-mat/0504173.
- [80] Y. Deng, Bulk and surface phase transitions in the three-dimensional O(4) spin model, *Phys. Rev. E* **73**, 056116 (2006).
- [81] www.gauss-centre.eu.
- [82] O. Vasilyev, A. Gambassi, A. Maciołek, and S. Dietrich, Monte Carlo simulation results for critical Casimir forces, *EPL* **80**, 60009 (2007), arXiv:0708.2902 [cond-mat.stat-mech].
- [83] V. Dohm, Critical Casimir force in slab geometry with finite aspect ratio: Analytic calculation above and below T_c , *EPL* **86**, 20001 (2009), arXiv:0902.2961 [cond-mat.stat-mech].
- [84] A. Hucht, D. Grüneberg, and F. M. Schmidt, Aspect-ratio dependence of thermodynamic Casimir forces, *Phys. Rev. E* **83**, 051101 (2011), arXiv:1012.4399 [cond-mat.stat-mech].
- [85] H. Hobrecht and A. Hucht, Critical Casimir force scaling functions of the two-dimensional Ising model at finite aspect ratios, *J. Stat. Mech.: Theory Exp.* **2** (2), 024002, arXiv:1611.05622 [cond-mat.stat-mech].
- [86] A. Hucht, The square lattice Ising model on the rectangle II: finite-size scaling limit, *J. Phys. A: Math. Theor.* **50**, 265205 (2017), arXiv:1701.08722 [math-ph].
- [87] H. Hobrecht and F. Hucht, Anisotropic scaling of the two-dimensional Ising model I: the Torus, *SciPost Physics* **7**, 026 (2019), arXiv:1803.10155 [cond-mat.stat-mech].
- [88] L. Cervellera, O. Oing, J. Büddefeld, and A. Hucht, The square lattice Ising model with quenched surface disorder, arXiv:2409.01434 [cond-mat.stat-mech].

End Matter

Appendix A: Scaling forms— Most of the scaling forms used in this work in order to fit the MC data are generalizations of those derived in the Supplemental Material of Ref. [5]. Here, we briefly recall the essential steps in this derivation. Lattice observables are generally expanded in terms of CFT fields belonging to the same symmetry sector. In particular, for bulk observables,

$$\begin{aligned} S(x) &= \mathcal{N}_S \left(1 + c_S \vec{\nabla}^2\right) \phi, \\ S^2(x) - \langle S^2(\vec{x}) \rangle &= \mathcal{N}_{S^2} \left(1 + c_{S^2} \vec{\nabla}^2\right) \epsilon, \\ E(x) - \langle E(\vec{x}) \rangle &= \mathcal{N}_E \left(1 + c_E \vec{\nabla}^2\right) \epsilon, \end{aligned} \quad (\text{A1})$$

where the constants \mathcal{N}_S , \mathcal{N}_{S^2} , \mathcal{N}_E , c_S , c_{S^2} , c_E are model-dependent. With this expansion, Eq. (10) follows immediately by taking the expectation value on a finite volume. Moreover, the finite-size amplitude U_E is given by $U_E = \mathcal{N}_E u_\epsilon$, where u_ϵ is the universal finite-size amplitude of the energy operator,

$$\langle \epsilon \rangle = \frac{u_\epsilon}{L^{\Delta_\epsilon}}. \quad (\text{A2})$$

We notice that, using Eq. (A1), one can in principle expect an additional correction $\propto L^{-2-\Delta_\epsilon}$ to the right-hand side of Eq. (10): our fit analysis shows that such a term is negligible

within the precision of MC data. Given that also S^2 couples to the energy operator, a finite-size scaling form for $S_{\text{bulk}}^2 \equiv (1/V) \sum_x S_x^2$ analogous to Eq. (10) holds

$$S_{\text{bulk}}^2 = S_0^2 + U_{S^2} L^{-\Delta_\epsilon}, \quad (\text{A3})$$

where $U_{S^2} = \mathcal{N}_{S^2} u_\epsilon$.

Using the bulk OPEs $\phi \times \phi = \lambda_{\phi\phi\epsilon} \epsilon$, and $\epsilon \times \epsilon = \lambda_{\epsilon\epsilon\epsilon} \epsilon$, one obtains Eq. (11) and Eq. (12) [5], as well as an analogous formula for the correlations of S^2 ,

$$\langle S_x^2 S_0^2 \rangle_c = \frac{\mathcal{N}_{S^2}^2}{x^{2\Delta_\epsilon}} \left[1 + B_{\epsilon\epsilon} \left(\frac{x}{L}\right)^{\Delta_\epsilon} + Cx^{-2} \right]. \quad (\text{A4})$$

We notice that the subleading correction $\propto (x/L)^{2\Delta_\epsilon}$ in Eq. (12) is due to the fact that we consider the connected part of the correlations: such a term is absent in Eq. (11). In principle, a subleading term $\propto (x/L)^{2\Delta_\epsilon}$ is also present in Eq. (A4): due to a reduced precision of the S^2 correlations, our analysis shows that such a correction is not relevant [65]. In Eqs. (11), (12), (A4), the finite-size coefficients are related to the OPE constants by

$$\begin{aligned} B_{\phi\phi} &= \lambda_{\phi\phi\epsilon} u_\epsilon, \\ B_{\epsilon\epsilon} &= \lambda_{\epsilon\epsilon\epsilon} u_\epsilon. \end{aligned} \quad (\text{A5})$$

Moreover, the subleading amplitude $B'_{\epsilon\epsilon}$ is related to the finite-size amplitude of the energy by $B'_{\epsilon\epsilon} = -u_\epsilon^2$, which holds within the available numerical precision. Combining the expansion (A1) with the BOPE (4) we derive in Ref. [5] Eq. (21) and show that $A_\phi = \mathcal{N}_S a_\phi$. The scaling form of the energy profile (16) follows analogously, and we have $A_\epsilon = (2/3)\mathcal{N}_E a_\epsilon$; here, as in Eq. (16), the factor 2/3 is due to the fact that in the definition of energy profile [Eq. (14)] we sum over 2 lattice directions, as opposed to the definition for the bulk observable [Eq. (9)], where the sum is over all 3 directions. Further, the finite-size correction is related to BOPEs as $B_\epsilon = 2^{\Delta_O} b_{\epsilon O} u_O / a_\epsilon$, with u_O the universal finite-size amplitude of the leading boundary operator O in Eq. (2):

$$\langle O \rangle = \frac{u_O}{L^{\Delta_O}}. \quad (\text{A6})$$

The profile of the S^2 observable, begin coupled to the energy operator [Eq. (A1)] satisfies a scaling form identical to Eq. (16)

$$\begin{aligned} \langle S_{\mathbf{x},z}^2 \rangle &= S_0^2 \\ &+ \frac{A_{S^2}}{(2(z+z_0))^{\Delta_\epsilon}} \left[1 + B_\epsilon \left(\frac{z+z_0}{L} \right)^{\Delta_\epsilon} + C(z+z_0)^{-2} \right], \end{aligned} \quad (\text{A7})$$

with S_0^2 extracted by Eq. (A3). Analogous to the above discussion, we have $A_{S^2} = \mathcal{N}_{S^2} a_\epsilon$. We notice that B_ϵ in Eq. (16) and Eq. (A7) are the same universal amplitude. At the special transition, the observable S^2 on the surface couples to the \mathbb{Z}_2 -even operator ε , hence its surface average $S_{\text{surf}}^2 \equiv (1/L^2) \sum_{\vec{x}} \langle S_{\vec{x},0}^2 \rangle$ satisfies a finite-size behavior analogous to Eq. (19)

$$S_{\text{surf}}^2 = \Sigma_0 + U_{\sigma^2} L^{-\Delta_\varepsilon}. \quad (\text{A8})$$

Correlations involving surface quantities follow from a similar expansion of the lattice observables in boundary CFT fields:

$$\begin{aligned} S(\mathbf{x}, 0) &= \mathcal{N}_\sigma \left(1 + c_\sigma \vec{\nabla}^2 \right) \phi, \\ S^2(\mathbf{x}, 0) - \langle S^2(\mathbf{x}, 0) \rangle &= \mathcal{N}_{\sigma^2} \left(1 + c_{\sigma^2} \vec{\nabla}^2 \right) \varepsilon, \\ E(\mathbf{x}, 0) - \langle E(\mathbf{x}, 0) \rangle &= \mathcal{N}_\varepsilon \left(1 + c_\varepsilon \vec{\nabla}^2 \right) \varepsilon. \end{aligned} \quad (\text{A9})$$

From this expansion and the OPE of $\sigma \times \sigma$, it follows that $B_{\sigma\sigma}$ in Eq. (15) is related to the OPE coefficient $\lambda_{\sigma\sigma O}$ by

$$B_{\sigma\sigma} = \lambda_{\sigma\sigma O} u_O, \quad (\text{A10})$$

where $O = D$, the displacement operator in the ordinary and in the normal UC, and $O = \varepsilon$ the relevant boundary \mathbb{Z}_2 -even operator in the special UC. Further, using Eq. (A9) one obtains Eq. (20) and an analogous scaling form for the two-point function of S^2 on the surface at the special UC

$$\langle S_{\mathbf{x},0}^2 S_{\mathbf{0},0}^2 \rangle = \frac{\mathcal{N}_{\sigma^2}^2}{x^{2\Delta_\varepsilon}} \left[1 + B_{\varepsilon\varepsilon} \left(\frac{x}{L} \right)^{\Delta_\varepsilon} + Cx^{-2} \right]. \quad (\text{A11})$$

We notice that the $B_{\varepsilon\varepsilon}$ in Eq. (20) and Eq. (A11) are the same amplitude, related to the OPE coefficient $\lambda_{\varepsilon\varepsilon\varepsilon}$ by

$$B_{\varepsilon\varepsilon} = \lambda_{\varepsilon\varepsilon\varepsilon} u_\varepsilon, \quad (\text{A12})$$

where u_ε is the universal finite-size amplitude of ε [See Eq. (A6)]. Finally, the scaling behavior of the surface-bulk correlation (17) follows from Eq. (A1) and Eq. (5), with $M_{\phi\sigma} = b_{\phi\sigma} 2^{\Delta_\sigma - \Delta_\phi} \mathcal{N}_S \mathcal{N}_\sigma$ and $B_{\phi\sigma} = \beta_{\phi\sigma O} u_O$ [5].

Appendix B: Critical Casimir amplitude— Given a three-dimensional system $L_\parallel \times L_\parallel \times L$ with lateral size L_\parallel , the critical Casimir force F_C is defined by

$$F_C \equiv - \left. \frac{\partial \left[L \left(\mathcal{F}^{(s)} - f_{\text{bulk}}^{(s)} \right) \right]}{\partial L} \right|_{L_\parallel, T}, \quad (\text{B1})$$

where $\mathcal{F}^{(s)}$ is the singular part of the free energy per volume $L_\parallel^2 L$ and in units of $k_B T$, and $f_{\text{bulk}}^{(s)}$ its thermodynamic limit $f_{\text{bulk}}^{(s)} = \lim_{L_\parallel, L \rightarrow \infty} \mathcal{F}^{(s)}$. At a critical point $T = T_c$ and for homogeneous BCs, or in the absence of a relevant length,

$$F_C = \frac{\Theta}{L^3}. \quad (\text{B2})$$

At the critical point, $\mathcal{F}^{(s)}(T = T_c) = A/L^3$. The critical Casimir amplitude Θ is related to the finite-size amplitude A of $\mathcal{F}^{(s)}$ by $\Theta = 2A$.

To compute the critical Casimir amplitude we employ the so-called coupling-parameter approach [82]. In essence, this consists in a combination of MC sampling and a numerical integration, yielding the free energy difference between a systems with thicknesses L and $L-1$, and identical lateral sizes. We refer to Refs. [46, 59] for a discussion on the implementation. For the numerical integration we use the Gauss-Kronrod method with 41/20 nodes, allowing for an accurate convergence of the integral; by comparing the resulting quadrature with 41 and 20 nodes we checked that the systematic error of the quadrature is negligible with respect to the statistical error bar. The free energy difference $I(L)$ at criticality is then fitted to

$$I(L) = F_{\text{bulk}}(\beta_c) + \frac{\Theta}{(L-1/2)^3} + \frac{C}{(L-1/2)^4}, \quad (\text{B3})$$

where $F_{\text{bulk}}(\beta_c)$ is the bulk free energy density at criticality, Θ is the desired Casimir amplitude, and the last term is due to $1/L$ scaling corrections. We note that for the BCs considered here, previous MC studies have considered the limit of infinite lateral size L_\parallel , whereas in this work we have chosen a geometry with equal sizes on all directions. Indeed, like any other FSS quantity, the Casimir amplitude depends on the aspect ratio $\rho = L/L_\parallel$ of the system. The dependence on ρ for three-dimensional models in the Ising universality class and periodic BCs has been studied in Ref. [83] with field-theoretical methods, and in Ref. [84] with MC simulations. Furthermore, the aspect-ratio dependence has been investigated for nonhomogeneous BCs, in the presence of a chemical step, and in the

TABLE B.I. Fits of the critical Casimir amplitude [Eq. (B3)] as a function of the minimum lattice size L_{\min} taken into account, for three BCs considered here; d.o.f. denotes the number of degrees of freedom of a fit.

BCs: (o,o)				
L_{\min}	$F_{\text{bulk}}(\beta_c)$	Θ	C	$\chi^2/\text{d.o.f.}$
8	0.075736842(44)	0.3005(14)	-0.184(11)	0.8
12	0.075736839(51)	0.3009(37)	-0.189(44)	1.1
16	0.075736895(57)	0.2907(66)	-0.01(11)	0.1
BCs: (+,o)				
L_{\min}	$F_{\text{bulk}}(\beta_c)$	Θ	C	$\chi^2/\text{d.o.f.}$
8	0.075737047(23)	0.5818(11)	-1.1665(89)	20.9
12	0.075736947(25)	0.5959(19)	-1.382(26)	1.9
16	0.075736923(29)	0.6013(34)	-1.496(64)	1.0
BCs: (+,+)				
L_{\min}	$F_{\text{bulk}}(\beta_c)$	Θ	C	$\chi^2/\text{d.o.f.}$
8	0.075736644(41)	-0.7794(16)	1.561(13)	2.7
12	0.075736715(47)	-0.7896(37)	1.695(45)	0.5
16	0.075736740(54)	-0.7945(65)	1.78(11)	0.3

limit $\rho \rightarrow 0$ in Refs. [46, 60]. In this situation, the chemical step forms a line defect and gives rise to a linear ρ dependence of the critical Casimir force on ρ , for $\rho \rightarrow 0$, allowing to extract its contribution to the Casimir force. In two dimensions, the aspect-ratio dependence of the Casimir force in Ising models with various BCs has been investigated in Refs. [85–88].

For three of the BCs studied here, we have computed $I(L)$ for lattice sizes $L = 8, 12, 16, 24, 32, 48, 64$. Corresponding fits to Eq. (B3) are reported in Table B.I. Inspecting the fit results we infer the following estimates of the critical Casimir amplitude Θ :

$$\Theta = 0.301(4) \quad (o, o) \text{ BCs,} \quad (\text{B4})$$

$$\Theta = 0.601(4) \quad (+, o) \text{ BCs,} \quad (\text{B5})$$

$$\Theta = -0.790(4) \quad (+, +) \text{ BCs.} \quad (\text{B6})$$

As noted above, all these amplitude pertain a model with aspect ratio $\rho = 1$. Interestingly, for (o, o) BCs we obtain a positive, i.e., repulsive critical Casimir amplitude. This is in stark contrast with slab limit $\rho = 0$, where the amplitude is negative $\Theta = -0.030(5)$ [59]. For $(+, o)$ BCs Θ is significantly larger than for $\rho = 0$, where $\Theta = 0.492(5)$ [59]. In the case of $(+, +)$ BCs we find instead that the critical Casimir amplitude Θ is rather close to the $\rho = 0$ limit, where $\Theta = -0.820(15)$ [57]. The data in Table B.I allows us to estimate the critical bulk free energy density. Considering the spread in the fitted values for different BCs, we conservatively estimate $F_{\text{bulk}}(\beta_c) = 0.075\,736\,8(1)$, improving the estimate $F_{\text{bulk}}(\beta_c) = 0.075\,736\,8(4)$ of Ref. [57].

Supplemental Material

ADDITIONAL RESULTS

As we discuss in Appendix A, both lattice observables E_x , defined in Eq. (9) and S^2 couple to the energy operator ϵ , hence the analysis of the OPE coefficients involving ϵ can be repeated using S^2 . In Table S.I we report estimates of the amplitudes extracted from fits of MC data involving the S^2 observable, for the bulk and boundary UCs discussed in this work. We observe that universal finite-size amplitudes $B_{\epsilon\epsilon}$, B_ϵ , $B_{\epsilon\epsilon}$ are in nice agreement with the estimates of Table II, thus underscoring the reliability of the results. Furthermore, for all surface UC the fitted value of z_0 matches that of Table II: as expected, z_0 is a model-dependent amplitude, which, for a given model, is independent of the observable [5].

Using the amplitudes related to S^2 we obtain alternative estimates of some of the universal coefficients discussed in the text. For the bulk UC, we compute $u_\epsilon = 3.216(8)$ and $\lambda_{\epsilon\epsilon\epsilon} = 1.52(3)$. For the ordinary UC we obtain $a_\epsilon = -0.757(6)$, $C_D = 0.0102(3)$, $u_D = 2.98(5)$, $b_{\epsilon D} = -0.84(2)$. For the special UC we extract $a_\epsilon = 1.159(5)$, $u_\epsilon = 1.74(2)$, $b_{\epsilon\epsilon} = 3.09(5)$, $\lambda_{\epsilon\epsilon\epsilon} = 1.01(2)$. For the normal UC, as realized with $(+, o)$ BCs, we obtain $a_\epsilon = 6.67(1)$, $u_D = 1.34(2)$, $C_D = 0.200(6)$; employing the latter in Eqs. (24)-(25), we obtain $b_{\epsilon D} = 1.68(3)$ and $b_{\phi D} = 0.241(4)$. All these results are in full agreement with those in Table I, obtained using the energy observable.

Moreover, as mentioned in the main text, we have also realized the normal UC by setting an infinite field on both surface $h_\uparrow = h_\downarrow = \infty$, i.e., with $(+, +)$ BCs. Together with the critical Casimir amplitude Θ_{++} determined in App. B, this set of simulations provides an independent set of estimates of the various universal BOPE coefficients. Following the same procedure, in Table S.I we report the fitted amplitudes. We

TABLE S.I. Estimates of amplitudes involving the S^2 observable, as well as those obtained with $(+, +)$ BCs.

UC	Fit results		Eq.
bulk	$S_0^2 = 0.6070252(7)$	$U_{S^2} = 0.2573(5)$	(A3)
	$\mathcal{N}_{S^2}^2 = 0.00640(2)$	$B_{\epsilon\epsilon} = 4.9(1)$	(A4)
ordinary	$A_{S^2} = -0.0606(5)$	$B_\epsilon = -26.6(8)$	(A7)
	$z_0 = 1.04(5)$		
special	$A_{S^2} = 0.0927(4)$	$B_\epsilon = 5.93(8)$	(A7)
	$z_0 = 0.51(2)$		
	$\Sigma_0 = 0.669447(1)$	$U_{\sigma^2} = 0.231(2)$	(A8)
	$\mathcal{N}_{\sigma^2}^2 = 0.0176(2)$	$B_{\epsilon\epsilon} = 1.76(3)$	(A11)
normal $(+, o)$	$A_{S^2} = 0.5339(5)$	$B_\epsilon = -2.70(8)$	(A7)
	$A_\epsilon = 4.838(6)$	$B_\epsilon = 3.6(1)$	(16)
normal $(+, +)$	$A_{S^2} = 0.5342(7)$	$B_\epsilon = 3.6(1)$	(A7)
	$z_0 = 1.44(2)$		
	$A_\phi = 1.1268(2)$	$B_\phi = 1.32(3)$	(21)
	$z_0 = 1.455(5)$		

TABLE S.II. Fits of surface two-point function at half-lattice distance in the special UC to Eq. (S1), as a function of the minimum lattice size L_{\min} taken into account. In the upper part of the table we fit the data ignoring the scaling-correction term cL^{-1} .

L_{\min}	A	$\hat{\Delta}_\sigma$	c	$\chi^2/\text{d.o.f.}$
32	0.99848(84)	0.353877(91)		1.87
48	0.9965(12)	0.35369(12)		1.05
64	0.9951(15)	0.35355(15)		0.66
96	0.9935(20)	0.35341(19)		0.39
32	0.9896(31)	0.35310(28)	0.135(46)	0.49
48	0.9884(49)	0.35300(42)	0.161(95)	0.59
64	0.9905(69)	0.35318(58)	0.11(16)	0.72

estimate $a_\phi = 2.6151(7)$, $a_\epsilon = 6.683(9)$ (using the energy observable), $a_\epsilon = 6.68(1)$ (using the S^2 observable). The universal norm C_D and the finite-size amplitude u_D are found $C_D = 0.197(6)$, $u_D = 1.78(3)$ [using the energy observable in Eq. (24)], $C_D = 0.197(5)$, $u_D = 1.78(2)$ [using Eq. (25)], $C_D = 0.197(6)$, $u_D = 1.78(3)$ [using the S^2 observable in Eq. (24)]. Using any of these values for C_D , we obtain $b_{\epsilon D} = 1.69(2)$ and $b_{\phi D} = 0.243(3)$. All these estimates are perfectly consistent with each other, and in full agreement with the estimates of Table I obtained with the $(+, o)$ BCs, thus underscoring the reliability of our results.

CRITICAL EXPONENT AT THE SPECIAL TRANSITION

Using the MC data we improve the critical exponent of the surface magnetization at the special transition. By standard FSS technique, we fit the two-point function of the surface at midsize distance $L/2$ to

$$\langle S_{L/2,0,0} S_{0,0} \rangle = AL^{-2\hat{\Delta}_\sigma} (1 + cL^{-1}), \quad (\text{S1})$$

leaving A , $\hat{\Delta}_\sigma$ and c as free parameters. Fit results are reported in Table S.II. In Eq. (S1) we have included the expected leading scaling correction $\propto L^{-1}$ arising from the irrelevant displacement operator. To monitor the relevance of the corrections we have repeated the fits setting $c = 0$. From the results of Table S.II we infer the estimate reported in Eq. (18), in agreement but more precise than a previous estimate $\hat{\Delta}_\sigma = 0.3535(6)$ [68].

TABLES OF FITS

In this section we provide the tables of fits used to extract the various amplitudes. As discussed in Ref. [5], to correctly take into account the statistical correlation in the MC data, we employ the Jackknife method [64] in the fits. We generally vary the critical exponents and other parameters employed in

TABLE S.III. Fit of E_{bulk} to Eq. (10), as a function of the minimum lattice size L_{min} taken into account. The quoted error bars are the sum of the statistical uncertainty obtained from the fit procedure and the variation of the fitted parameters on varying the exponent $\Delta_\epsilon = 1.412625(10)$ [66] within one error bar.

L_{min}	E_0	U_E	$\chi^2/\text{d.o.f.}$
32	1.2042336(80)	3.4956(58)	0.5
48	1.2042334(88)	3.4958(76)	0.6
64	1.2042348(98)	3.4938(98)	0.8
96	1.2042404(120)	3.4844(152)	0.8
128	1.2042278(174)	3.51(30)	0.7

the fits by the quoted error bars, and sum the resulting variation in the fitted parameters to the statistical error of the fit. Under such a variation, the minimum $\chi^2/\text{d.o.f.}$ of the fits may change significantly. In this case, we quote an uncertainty to the minimum $\chi^2/\text{d.o.f.}$, reflecting this variation.

In Tables S.III and S.IV we report fit results of bulk observables E_{bulk} and S_{bulk}^2 to Eq. (10) and Eq. (A3), respectively. In Tables S.V, S.VI, S.VIII we report the fits of the two-point functions of bulk observables. In Table S.VI we have fitted the energy correlations to Eq. (12) setting $B'_{\epsilon\epsilon} = 0$, i.e., considering the leading finite-size correction only. We have observed a somewhat large residual $\chi^2/\text{d.o.f.}$ in the fits, and a small drift in the fitted values of $B_{\epsilon\epsilon}$. Including the next-to-leading correction $\propto (x/L)^{2\Delta_\epsilon}$ significantly improve the quality of the fits, leading to a good $\chi^2/\text{d.o.f.}$ for $(x/L)_{\text{max}} = 1/8$. Nevertheless, the additional coefficient $B'_{\epsilon\epsilon}$ is rather unstable with respect to the maximum value of (x/L) used in the fits: we have therefore quoted in Table II a rather conservative estimate for it. For the fitted amplitude $B_{\epsilon\epsilon}$ we quote an uncertainty compatible with the fits obtained for $x_{\text{min}} = 6$ and $x_{\text{min}} = 8$. Due to a reduced precision, fits of the S^2 correlations do not necessitate the additional correction term $\propto (x/L)^{2\Delta_\epsilon}$.

In Tables S.IX-S.XIV we report fits pertaining to the ordinary UC. In the fits of the energy and S^2 profile to Eq. (16) and Eq. (A7) (Tables S.X and S.XII) we observed that the fitted coefficient C vanishes within error bars. Therefore we have repeated the fits setting $C = 0$ (Tables S.XI and S.XIII).

In Tables S.XV-S.XXV we report fits pertaining to the special UC. In the fits of the surface two-point function of the order parameter to Eq. (15) (Table S.XV), of the energy profile to Eq. (16) (Table S.XVII), and of the S^2 profile to Eq. (A7) (Table S.XIX) we observed that the fitted coefficient C vanishes within error bars. As for the ordinary UC, we report in Tables S.XVI, S.XVIII, S.XX fits setting $C = 0$.

In Tables S.XXVI-S.XXXII we report fits pertaining to the normal UC. In the case of $(+, +)$, fits of the order parameter profile to Eq. (21) reported in Table S.XXXI give a rather small coefficient C , marginally compatible with 0. As in previous cases, we report in Table S.XXXII fits setting $C = 0$.

TABLE S.IV. Same as Table S.III for the fits of S_{bulk}^2 to Eq. (A3).

L_{min}	S_0^2	U_{S^2}	$\chi^2/\text{d.o.f.}$
32	0.60702515(63)	0.25726(46)	0.5
48	0.60702515(69)	0.25726(60)	0.7
64	0.60702540(76)	0.25689(76)	0.7
96	0.60702583(94)	0.2562(12)	0.7
128	0.6070248(14)	0.2583(23)	0.4

TABLE S.V. Fits of the two-point function of bulk observable S to Eq. (11), as a function of the minimum distance x_{\min} , the maximum value $(x/L)_{\max}$, and the minimum lattice size L_{\min} considered in the fits. Variation of the critical exponent $\Delta_\phi = 0.518\,148\,9(10)$ [66] within its uncertainty gives a rather small contribution to the uncertainty.

x_{\min}	$(x/L)_{\max}$	L_{\min}	\mathcal{N}_S^2	$B_{\phi\phi}$	C	$\chi^2/\text{d.o.f.}$
4	$\frac{1}{4}$	32	0.185359(33)	3.4220(32)	0.3382(29)	5.64
		48	0.185337(32)	3.4261(38)	0.3405(28)	5.16
		64	0.185320(29)	3.4301(42)	0.3426(25)	4.67
		96	0.185304(24)	3.4353(53)	0.3448(21)	3.97
		128	0.185286(19)	3.4482(76)	0.3475(16)	1.99
	$\frac{1}{8}$	32	0.185431(36)	3.3976(47)	0.3347(29)	7.18
		48	0.185421(37)	3.4000(53)	0.3356(30)	7.15
		64	0.185399(36)	3.4063(57)	0.3374(29)	7.02
		96	0.185360(34)	3.4187(70)	0.3407(28)	6.6
		128	0.185282(28)	3.4508(92)	0.3477(23)	3.77
6	$\frac{1}{4}$	32	0.185548(61)	3.4147(39)	0.278(12)	2.19
		48	0.185542(61)	3.4152(44)	0.279(12)	2.16
		64	0.185528(57)	3.4170(47)	0.283(11)	2.06
		96	0.185508(51)	3.4198(56)	0.289(10)	1.83
		128	0.185452(40)	3.4329(76)	0.3047(80)	0.67
	$\frac{1}{8}$	48	0.185656(64)	3.3864(67)	0.269(11)	0.84
		64	0.185656(65)	3.3864(72)	0.269(11)	0.86
		96	0.185653(68)	3.3871(92)	0.269(12)	0.9
		128	0.185560(67)	3.409(12)	0.287(12)	0.3
		8	$\frac{1}{4}$	32	0.185568(92)	3.4171(50)
48	0.185577(93)			3.4161(54)	0.246(32)	1.71
64	0.185573(91)			3.4163(57)	0.249(32)	1.69
96	0.185554(86)			3.4179(67)	0.259(30)	1.58
128	0.185442(72)			3.4340(84)	0.309(26)	0.64
$\frac{1}{8}$	64		0.185716(96)	3.3852(92)	0.231(28)	0.46
	96		0.18572(10)	3.384(11)	0.228(31)	0.46
	128		0.18562(12)	3.403(17)	0.262(37)	0.18

TABLE S.VI. Fits of the two-point function of bulk observable E to Eq. (12), fixing $B'_{\epsilon\epsilon} = 0$, as a function of the minimum distance x_{\min} , the maximum value $(x/L)_{\max}$, and the minimum lattice size L_{\min} considered in the fits. Variation of the critical exponent $\Delta_\epsilon = 1.412625(10)$ [66] within its uncertainty gives a rather small contribution to the uncertainty.

x_{\min}	$(x/L)_{\max}$	L_{\min}	\mathcal{N}_E^2	$B_{\epsilon\epsilon}$	C	$\chi^2/\text{d.o.f.}$	
4	$\frac{1}{4}$	32	1.17834(37)	4.6515(84)	1.3622(43)	24.78	
		48	1.17830(38)	4.663(10)	1.3602(45)	21.78	
		64	1.17822(39)	4.683(12)	1.3567(46)	17.34	
		96	1.17821(42)	4.707(18)	1.3497(49)	12.09	
		128	1.17745(45)	4.789(28)	1.3498(51)	7.74	
	$\frac{1}{8}$	32	1.17598(38)	4.8248(94)	1.3792(43)	20.79	
		48	1.17611(39)	4.818(11)	1.3776(46)	20.96	
		64	1.17609(41)	4.829(13)	1.3758(47)	17.95	
		96	1.17618(44)	4.844(19)	1.3705(52)	13.73	
		128	1.17555(48)	4.928(30)	1.3710(55)	9.11	
	$\frac{1}{12}$	48	1.17460(39)	4.963(13)	1.3865(44)	16.6	
		64	1.17476(41)	4.953(15)	1.3845(46)	16.8	
		96	1.17495(47)	4.949(21)	1.3809(53)	14.9	
		128	1.17391(54)	5.064(34)	1.3878(61)	8.8	
	6	$\frac{1}{4}$	32	1.18596(65)	4.490(10)	1.147(17)	7.12
48			1.18566(67)	4.501(12)	1.154(17)	7.09	
64			1.18532(71)	4.521(15)	1.156(18)	6.33	
96			1.18521(78)	4.542(21)	1.145(19)	4.84	
128			1.18496(87)	4.581(33)	1.125(21)	3.0	
$\frac{1}{8}$		48	1.18318(70)	4.649(14)	1.176(17)	4.36	
		64	1.18291(74)	4.659(17)	1.183(18)	4.32	
		96	1.18273(82)	4.671(23)	1.184(20)	3.97	
		128	1.18229(96)	4.715(37)	1.181(23)	2.63	
		96	1.18140(82)	4.778(25)	1.192(19)	1.83	
$\frac{1}{12}$		128	1.1802(11)	4.848(45)	1.215(25)	0.84	
		32	1.18969(99)	4.410(13)	0.995(45)	3.38	
8		$\frac{1}{4}$	48	1.1898(10)	4.408(14)	0.991(46)	3.39
			64	1.1891(11)	4.428(18)	1.017(50)	3.27
			96	1.1887(12)	4.449(25)	1.010(54)	2.8
	128		1.1887(14)	4.480(40)	0.959(61)	2.0	
	64		1.1863(11)	4.571(21)	1.044(50)	2.23	
	$\frac{1}{8}$	96	1.1860(13)	4.580(27)	1.057(54)	2.24	
		128	1.1851(16)	4.622(47)	1.071(66)	1.76	
		96	1.1840(12)	4.715(33)	1.060(51)	0.54	
	$\frac{1}{12}$	128	1.1827(17)	4.766(57)	1.113(67)	0.32	

TABLE S.VII. Fits of the two-point function of bulk observable E to Eq. (12), including the correction term $B'_{\epsilon\epsilon}(x/L)^{2\Delta_\epsilon}$, as a function of the minimum distance x_{\min} , the maximum value $(x/L)_{\max}$, and the minimum lattice size L_{\min} considered in the fits. Variation of the critical exponent $\Delta_\epsilon = 1.412625(10)$ [66] within its uncertainty gives a rather small contribution to the uncertainty.

x_{\min}	$(x/L)_{\max}$	L_{\min}	\mathcal{N}_E^2	$B_{\epsilon\epsilon}$	$B'_{\epsilon\epsilon}$	C	$\chi^2/\text{d.o.f.}$	
4	$\frac{1}{4}$	32	1.17426(40)	5.015(14)	-4.65(14)	1.3933(45)	8.36	
		48	1.17441(42)	5.029(16)	-5.25(17)	1.3888(47)	6.77	
		64	1.17450(43)	5.037(18)	-5.47(22)	1.3857(49)	5.75	
		96	1.17466(48)	5.045(25)	-5.65(32)	1.3808(54)	4.85	
		128	1.17369(56)	5.164(40)	-6.84(55)	1.3866(62)	3.54	
	$\frac{1}{8}$	32	1.17275(42)	5.191(22)	-8.16(38)	1.4030(46)	11.35	
		48	1.17266(42)	5.256(21)	-10.56(41)	1.3991(47)	7.94	
		64	1.17304(44)	5.240(23)	-10.69(49)	1.3937(48)	7.35	
		96	1.17338(51)	5.219(32)	-10.41(67)	1.3887(55)	6.94	
		128	1.17230(66)	5.341(56)	-11.8(1.3)	1.3982(68)	5.15	
	$\frac{1}{12}$	48	1.17252(47)	5.277(36)	-11.1(1.0)	1.3998(48)	13.35	
		64	1.17242(47)	5.347(35)	-14.8(1.0)	1.3971(49)	11.77	
		96	1.17301(53)	5.293(38)	-13.6(1.1)	1.3902(55)	11.26	
		128	1.17257(71)	5.285(67)	-9.0(2.0)	1.3969(71)	8.14	
		6	$\frac{1}{4}$	32	1.18150(74)	4.773(21)	-2.94(18)	1.209(18)
48	1.18124(76)			4.815(22)	-3.67(22)	1.205(18)	1.91	
64	1.18103(79)			4.836(25)	-4.01(26)	1.205(19)	1.72	
96	1.18110(87)			4.846(31)	-4.26(35)	1.198(20)	1.58	
128	1.1804(11)			4.911(53)	-4.92(62)	1.204(25)	1.24	
$\frac{1}{8}$	48		1.17907(82)	5.011(39)	-7.14(65)	1.226(18)	1.17	
	64		1.17899(82)	5.040(40)	-8.03(75)	1.222(19)	0.95	
	96		1.17913(89)	5.064(44)	-9.11(88)	1.211(20)	0.74	
	128		1.1782(13)	5.124(77)	-9.9(1.6)	1.229(26)	0.68	
	96		1.17867(99)	5.128(74)	-11.2(2.1)	1.213(20)	0.67	
$\frac{1}{12}$	128		1.1784(13)	5.09(10)	-8.4(2.9)	1.228(26)	0.43	
8	$\frac{1}{4}$		32	1.1848(12)	4.651(29)	-2.17(22)	1.112(49)	1.85
			48	1.1844(12)	4.695(31)	-2.77(26)	1.098(49)	1.38
			64	1.1841(12)	4.723(32)	-3.14(31)	1.102(51)	1.29
			96	1.1840(14)	4.738(39)	-3.40(40)	1.095(56)	1.26
		128	1.1831(18)	4.798(70)	-3.98(72)	1.104(70)	1.10	
	$\frac{1}{8}$	64	1.1805(14)	4.990(68)	-7.5(1.1)	1.154(53)	0.79	
		96	1.1803(14)	5.048(71)	-9.0(1.4)	1.134(55)	0.59	
		128	1.1798(21)	5.08(11)	-9.5(2.0)	1.152(71)	0.64	
		96	1.1804(24)	5.05(19)	-9.0(4.6)	1.119(62)	0.27	
		128	1.1806(23)	4.99(18)	-6.5(4.9)	1.135(69)	0.21	

TABLE S.VIII. Same as Table S.VI for the fits of bulk S^2 correlations to Eq. (A4).

x_{\min}	$(x/L)_{\max}$	L_{\min}	$\mathcal{N}_{S^2}^2$	$B_{\epsilon\epsilon}$	C	$\chi^2/\text{d.o.f.}$	
4	$\frac{1}{4}$	32	0.0063737(35)	4.757(18)	1.3321(88)	2.38	
		48	0.0063715(36)	4.791(21)	1.3351(89)	2.18	
		64	0.0063695(38)	4.835(26)	1.3362(94)	1.98	
		96	0.0063697(41)	4.863(35)	1.3309(99)	1.59	
		128	0.0063688(51)	4.912(62)	1.328(12)	1.4	
	$\frac{1}{8}$	32	0.0063676(35)	4.866(22)	1.3383(89)	2.1	
		48	0.0063667(36)	4.876(25)	1.3401(90)	2.11	
		64	0.0063643(38)	4.918(29)	1.3432(94)	1.76	
		96	0.0063648(43)	4.940(39)	1.339(10)	1.33	
		128	0.0063627(53)	5.011(66)	1.338(12)	1.12	
	$\frac{1}{12}$	48	0.0063628(36)	4.975(27)	1.3417(90)	1.33	
		64	0.0063609(39)	4.999(32)	1.3454(95)	1.29	
		96	0.0063625(44)	4.988(43)	1.341(10)	1.12	
		128	0.0063581(57)	5.096(76)	1.346(12)	0.84	
	6	$\frac{1}{4}$	32	0.0064211(90)	4.514(30)	1.132(48)	1.34
48			0.0064177(91)	4.537(34)	1.146(49)	1.33	
64			0.0064130(98)	4.573(43)	1.165(51)	1.36	
96			0.006407(11)	4.629(56)	1.184(54)	1.29	
128			0.006404(12)	4.653(85)	1.188(60)	1.24	
$\frac{1}{8}$		48	0.0064097(96)	4.641(45)	1.156(50)	1.08	
		64	0.006404(10)	4.683(49)	1.181(51)	1.02	
		96	0.006396(11)	4.743(62)	1.212(55)	0.99	
		128	0.006389(13)	4.803(91)	1.240(61)	0.94	
$\frac{1}{12}$		96	0.006394(11)	4.803(70)	1.205(56)	0.67	
		128	0.006380(13)	4.93(11)	1.263(61)	0.63	
		192	0.006357(22)	5.18(21)	1.358(92)	0.57	
8		$\frac{1}{4}$	32	0.006427(18)	4.477(49)	1.11(19)	1.31
			48	0.006427(18)	4.479(51)	1.12(19)	1.32
			64	0.006423(20)	4.494(65)	1.14(20)	1.36
	96		0.006420(21)	4.535(83)	1.14(20)	1.29	
	128		0.006436(24)	4.48(12)	0.93(22)	1.25	
	$\frac{1}{8}$	64	0.006402(22)	4.704(93)	1.18(20)	1.06	
		96	0.006400(23)	4.72(10)	1.19(21)	1.08	
		128	0.006405(27)	4.71(14)	1.12(23)	1.01	
	$\frac{1}{12}$	96	0.006395(24)	4.88(13)	1.09(21)	0.70	
		128	0.006383(29)	4.96(19)	1.18(24)	0.72	
		192	0.006316(42)	5.48(32)	1.63(31)	0.56	
	10	$\frac{1}{4}$	48	0.006455(29)	4.361(63)	0.87(48)	1.26
			64	0.006463(30)	4.330(73)	0.78(48)	1.27
			96	0.006462(36)	4.36(11)	0.72(55)	1.23
			128	0.006476(48)	4.34(17)	0.42(68)	1.27
$\frac{1}{8}$		96	0.006447(36)	4.55(12)	0.57(56)	1.05	
		128	0.006431(51)	4.65(20)	0.70(70)	1.08	

TABLE S.IX. Fits of the two-point function of surface order parameter S at the ordinary UC to Eq. (15), as a function of the minimum distance x_{\min} , the maximum value $(x/L)_{\max}$, and the minimum lattice size L_{\min} considered in the fits. The uncertainty due to the variation of the boundary scaling dimension $\hat{\Delta}_\sigma = 2 - 0.7249(6)$ [58] within one quoted error bar largely dominates over the statistical error bars of the fits. As a reference, a fit employing only the central value of $\hat{\Delta}_\sigma$ for $x_{\min} = 4$, $(x/L)_{\max} = 1/4$, $L_{\min} = 48$ results in $\mathcal{N}_\sigma^2 = 0.385279(25)$.

x_{\min}	$(x/L)_{\max}$	L_{\min}	\mathcal{N}_σ^2	$B_{\sigma\sigma}$	C	$\chi^2/\text{d.o.f.}$		
4	$\frac{1}{4}$	32	0.3853(11)	4.397(85)	-0.611(17)	44.0(6.8)		
		48	0.3853(11)	4.15(13)	-0.611(17)	44.0(6.7)		
		64	0.3853(11)	3.75(21)	-0.612(17)	44.4(6.7)		
		96	0.3853(11)	3.14(38)	-0.612(17)	45.1(6.7)		
		128	0.3853(11)	2.57(57)	-0.612(17)	47.3(7.0)		
	$\frac{1}{8}$	32	0.3853(11)	3.83(16)	-0.612(17)	92.0(14.0)		
		48	0.3853(11)	3.67(21)	-0.612(17)	93.0(14.0)		
		64	0.3853(11)	2.81(35)	-0.614(17)	93.0(14.0)		
		96	0.3854(11)	0.33(86)	-0.616(17)	91.0(14.0)		
		128	0.3854(11)	-2.3(1.5)	-0.617(17)	93.0(13.0)		
		6	$\frac{1}{4}$	32	0.3833(13)	4.723(62)	-0.404(44)	1.53(29)
				48	0.3834(13)	4.661(89)	-0.405(43)	1.45(27)
				64	0.3834(13)	4.54(15)	-0.406(43)	1.36(25)
				96	0.3834(13)	4.37(28)	-0.407(43)	1.26(23)
128	0.3834(13)			4.38(42)	-0.406(43)	1.34(25)		
$\frac{1}{8}$	48		0.3834(13)	4.34(19)	-0.408(43)	1.19(43)		
	64		0.3834(13)	4.31(24)	-0.408(43)	1.20(43)		
	96		0.3834(13)	4.23(56)	-0.408(43)	1.20(42)		
	128		0.3834(13)	4.0(1.0)	-0.409(42)	1.22(41)		
	8		$\frac{1}{4}$	32	0.3831(15)	4.778(63)	-0.348(87)	1.216(96)
				48	0.3831(15)	4.722(78)	-0.352(87)	1.172(91)
				64	0.3831(15)	4.61(13)	-0.356(87)	1.106(77)
				96	0.3832(15)	4.45(23)	-0.359(87)	1.015(61)
				128	0.3831(15)	4.50(35)	-0.357(86)	1.076(70)
$\frac{1}{8}$		64	0.3832(15)	4.37(30)	-0.364(86)	0.657(68)		
		96	0.3832(15)	4.32(49)	-0.365(87)	0.661(67)		
		128	0.3832(15)	4.26(86)	-0.367(87)	0.692(67)		

TABLE S.X. Fits of the energy profile at the ordinary UC to Eq. (16), as a function of the minimum distance z_{\min} from the surface, the maximum ratio $(z/L)_{\max}$, and the minimum lattice size L_{\min} considered in the fits. We employ the fitted value of E_0 reported in Table II. Varying E_0 within one error bar quoted in Table II results in a significant additional uncertainty in the results. As a reference, a fit employing only the central value of E_0 for $z_{\min} = 4$, $(z/L)_{\max} = 1/8$, $L_{\min} = 48$ results in $A_\epsilon = -0.54614(80)$.

z_{\min}	$(z/L)_{\max}$	L_{\min}	A_ϵ	z_0	B_ϵ	C	$\chi^2/\text{d.o.f.}$
4	$\frac{1}{4}$	32	-0.5446(33)	1.015(54)	-22.61(45)	0.20(25)	7.44(40)
		48	-0.5442(33)	1.008(55)	-22.57(47)	0.18(25)	6.11(46)
		64	-0.5438(32)	1.000(53)	-22.53(52)	0.13(25)	5.31(53)
		96	-0.5434(31)	0.990(50)	-22.42(63)	0.08(23)	4.85(54)
		128	-0.5429(29)	0.978(47)	-22.12(78)	0.02(21)	4.36(42)
		192	-0.5425(27)	0.966(42)	-21.6(1.0)	-0.04(18)	3.27(11)
	$\frac{1}{8}$	32	-0.5461(28)	1.031(44)	-26.80(69)	0.25(20)	1.25(27)
		48	-0.5461(28)	1.030(44)	-26.79(78)	0.25(20)	1.26(27)
		64	-0.5462(28)	1.031(44)	-26.82(88)	0.25(20)	1.28(28)
		96	-0.5468(29)	1.042(46)	-27.7(1.1)	0.31(21)	1.06(32)
		128	-0.5471(29)	1.048(46)	-28.2(1.4)	0.33(21)	1.09(37)
		192	-0.5465(27)	1.036(43)	-27.1(2.2)	0.28(19)	0.93(32)
6	$\frac{1}{4}$	32	-0.5447(46)	1.03(10)	-22.32(55)	0.41(69)	6.29(31)
		48	-0.5453(48)	1.05(11)	-22.42(55)	0.53(74)	5.80(30)
		64	-0.5452(49)	1.05(11)	-22.45(56)	0.54(77)	5.21(35)
		96	-0.5447(49)	1.03(11)	-22.42(62)	0.43(76)	4.85(41)
		128	-0.5433(47)	0.99(11)	-22.13(74)	0.13(67)	4.41(39)
		192	-0.5413(42)	0.929(89)	-21.54(96)	-0.31(53)	3.28(18)
	$\frac{1}{8}$	48	-0.5473(41)	1.069(87)	-26.60(86)	0.55(55)	1.17(14)
		64	-0.5474(41)	1.071(87)	-26.73(93)	0.56(56)	1.16(14)
		96	-0.5485(43)	1.096(92)	-27.8(1.1)	0.71(60)	0.82(14)
		128	-0.5493(45)	1.114(98)	-28.5(1.3)	0.83(64)	0.77(16)
		192	-0.5486(46)	1.10(10)	-27.9(2.0)	0.71(65)	0.71(17)
		8	$\frac{1}{4}$	32	-0.5446(57)	1.05(17)	-22.10(66)
48	-0.5458(60)			1.09(18)	-22.20(66)	1.1(1.5)	5.44(22)
64	-0.5466(64)			1.12(19)	-22.29(65)	1.3(1.7)	5.12(21)
96	-0.5466(68)			1.12(20)	-22.34(66)	1.3(1.8)	4.80(27)
128	-0.5444(66)			1.04(19)	-22.12(73)	0.6(1.6)	4.45(32)
192	-0.5401(58)			0.88(16)	-21.48(91)	-0.8(1.2)	3.32(25)
$\frac{1}{8}$	64		-0.5485(54)	1.11(14)	-26.9(1.1)	0.9(1.2)	1.147(97)
	96		-0.5494(55)	1.13(15)	-27.7(1.2)	1.1(1.2)	0.814(92)
	128		-0.5504(59)	1.16(16)	-28.4(1.3)	1.3(1.3)	0.722(90)
	192		-0.5499(64)	1.14(17)	-28.1(1.9)	1.2(1.4)	0.68(11)

TABLE S.XI. Same as Table S.X, fixing $C = 0$. A variation of E_0 within the uncertainty quoted in Table II gives a rather significant contribution to the final uncertainty of the fitted parameters. As a reference, a fit employing only the central value of E_0 for $z_{\min} = 4$, $(z/L)_{\max} = 1/8$, $L_{\min} = 48$ results in $A_\epsilon = -0.54396(32)$.

z_{\min}	$(z/L)_{\max}$	L_{\min}	A_ϵ	z_0	B_ϵ	$\chi^2/\text{d.o.f.}$
4	$\frac{1}{4}$	32	-0.5429(14)	0.9766(92)	-22.67(40)	7.84(82)
		48	-0.5428(13)	0.9750(88)	-22.57(47)	6.43(80)
		64	-0.5427(13)	0.9741(85)	-22.49(56)	5.54(76)
		96	-0.5426(12)	0.9735(80)	-22.36(72)	4.98(67)
		128	-0.5427(12)	0.9735(78)	-22.10(90)	4.44(45)
		192	-0.5429(12)	0.9746(78)	-21.7(1.1)	3.27(12)
	$\frac{1}{8}$	32	-0.5440(12)	0.9831(79)	-26.81(68)	2.01(87)
		48	-0.5440(12)	0.9828(78)	-26.68(84)	2.00(86)
		64	-0.5439(12)	0.9823(76)	-26.5(1.1)	2.01(85)
		96	-0.5440(11)	0.9827(72)	-26.8(1.5)	1.98(95)
		128	-0.5439(11)	0.9826(68)	-26.6(1.9)	2.08(98)
		192	-0.5438(10)	0.9814(64)	-25.1(2.7)	1.57(72)
6	$\frac{1}{4}$	32	-0.5431(22)	0.980(20)	-22.44(40)	6.56(60)
		48	-0.5432(21)	0.981(20)	-22.52(45)	6.15(66)
		64	-0.5430(21)	0.979(19)	-22.49(52)	5.54(69)
		96	-0.5428(20)	0.976(18)	-22.38(66)	5.07(65)
		128	-0.5427(19)	0.974(17)	-22.10(83)	4.50(45)
		192	-0.5428(18)	0.973(16)	-21.7(1.1)	3.34(11)
	$\frac{1}{8}$	48	-0.5449(19)	0.995(17)	-26.67(82)	1.60(52)
		64	-0.5449(19)	0.995(17)	-26.73(93)	1.61(53)
		96	-0.5452(19)	0.999(16)	-27.5(1.2)	1.45(62)
		128	-0.5453(18)	0.999(16)	-27.6(1.6)	1.53(67)
		192	-0.5449(17)	0.995(14)	-26.3(2.4)	1.20(52)
		8	$\frac{1}{4}$	32	-0.5430(30)	0.981(36)
48	-0.5434(30)			0.987(36)	-22.40(45)	5.75(55)
64	-0.5434(29)			0.987(35)	-22.47(50)	5.51(60)
96	-0.5432(28)			0.982(33)	-22.39(62)	5.13(61)
128	-0.5427(27)			0.975(31)	-22.10(78)	4.58(46)
192	-0.5424(25)			0.967(29)	-21.6(1.0)	3.43(13)
$\frac{1}{8}$	64		-0.5459(26)	1.013(29)	-27.03(98)	1.41(34)
	96		-0.5464(26)	1.019(30)	-27.8(1.1)	1.13(37)
	128		-0.5467(26)	1.023(30)	-28.3(1.4)	1.14(42)
	192		-0.5462(25)	1.015(28)	-27.3(2.1)	0.97(36)

TABLE S.XII. Fits of the S^2 profile at the ordinary UC to Eq. (A7), as a function of the minimum distance z_{\min} from the surface, the maximum ratio $(z/L)_{\max}$, and the minimum lattice size L_{\min} considered in the fits. We employ the fitted value of S_0^2 reported in Table S.I. Varying S_0^2 within one error bar quoted in Table S.I results in a significant additional uncertainty in the results. As a reference, a fit employing only the central value of S_0^2 for $z_{\min} = 4$, $(z/L)_{\max} = 1/4$, $L_{\min} = 32$ results in $A_{S^2} = -0.060223(80)$.

z_{\min}	$(z/L)_{\max}$	L_{\min}	A_{S^2}	z_0	B_ϵ	C	$\chi^2/\text{d.o.f.}$
4	$\frac{1}{4}$	32	-0.06022(42)	1.027(65)	-22.43(51)	0.45(31)	7.79(62)
		48	-0.06019(43)	1.022(65)	-22.41(53)	0.42(32)	6.50(70)
		64	-0.06015(42)	1.014(63)	-22.38(59)	0.38(30)	5.71(78)
		96	-0.06010(40)	1.004(59)	-22.26(71)	0.33(28)	5.25(80)
		128	-0.06004(37)	0.990(55)	-21.93(88)	0.26(25)	4.71(64)
		192	-0.05998(35)	0.976(49)	-21.4(1.2)	0.18(22)	3.46(22)
	$\frac{1}{8}$	32	-0.06038(35)	1.041(51)	-26.51(75)	0.48(24)	1.39(38)
		48	-0.06039(36)	1.042(51)	-26.56(84)	0.49(24)	1.40(39)
		64	-0.06039(36)	1.042(52)	-26.59(95)	0.49(24)	1.42(40)
		96	-0.06047(37)	1.054(53)	-27.5(1.2)	0.55(25)	1.20(45)
		128	-0.06050(37)	1.060(54)	-28.0(1.5)	0.58(26)	1.23(51)
		192	-0.06042(34)	1.046(49)	-26.7(2.3)	0.51(23)	1.05(45)
6	$\frac{1}{4}$	32	-0.06026(59)	1.06(12)	-22.13(63)	0.73(84)	6.64(46)
		48	-0.06035(62)	1.08(13)	-22.24(63)	0.88(90)	6.10(44)
		64	-0.06035(63)	1.08(13)	-22.29(64)	0.90(93)	5.51(50)
		96	-0.06030(63)	1.06(13)	-22.27(70)	0.80(92)	5.17(59)
		128	-0.06013(60)	1.02(12)	-21.96(82)	0.47(81)	4.72(56)
		192	-0.05989(53)	0.95(10)	-21.3(1.1)	-0.03(63)	3.46(30)
	$\frac{1}{8}$	48	-0.06054(51)	1.09(10)	-26.35(94)	0.85(65)	1.24(20)
		64	-0.06056(52)	1.09(10)	-26.5(1.0)	0.87(66)	1.23(20)
		96	-0.06069(54)	1.12(11)	-27.6(1.2)	1.03(70)	0.86(20)
		128	-0.06077(57)	1.13(11)	-28.3(1.4)	1.16(75)	0.81(22)
		192	-0.06069(58)	1.12(11)	-27.7(2.1)	1.02(76)	0.75(23)
		8	$\frac{1}{4}$	32	-0.06028(73)	1.09(19)	-21.91(75)
48	-0.06043(77)			1.13(20)	-22.01(75)	1.6(1.8)	5.72(32)
64	-0.06053(82)			1.16(22)	-22.10(75)	1.9(2.0)	5.36(31)
96	-0.06054(87)			1.17(24)	-22.16(75)	1.9(2.2)	5.04(38)
128	-0.06030(85)			1.08(23)	-21.95(82)	1.2(2.0)	4.71(45)
192	-0.05980(74)			0.91(18)	-21.3(1.0)	-0.4(1.4)	3.51(37)
$\frac{1}{8}$	64		-0.06071(67)	1.14(16)	-26.7(1.1)	1.4(1.4)	1.16(13)
	96		-0.06081(69)	1.16(17)	-27.5(1.3)	1.5(1.4)	0.82(12)
	128		-0.06092(73)	1.19(18)	-28.2(1.4)	1.7(1.5)	0.73(12)
	192		-0.06086(79)	1.17(19)	-27.9(2.0)	1.6(1.6)	0.69(15)

TABLE S.XIII. Same as Table S.XII, fixing $C = 0$. A variation of S_0^2 within the uncertainty quoted in Table S.I gives a rather significant contribution to the final uncertainty of the fitted parameters. As a reference, a fit employing only the central value of S_0^2 for $z_{\min} = 4$, $(z/L)_{\max} = 1/4$, $L_{\min} = 96$ results in $A_\epsilon = -0.059791(33)$.

z_{\min}	$(z/L)_{\max}$	L_{\min}	A_{S^2}	z_0	B_ϵ	$\chi^2/\text{d.o.f.}$	
4	$\frac{1}{4}$	32	-0.05983(17)	0.946(10)	-22.55(45)	9.2(1.7)	
		48	-0.05981(17)	0.9438(99)	-22.41(54)	7.7(1.7)	
		64	-0.05980(16)	0.9427(95)	-22.28(64)	6.7(1.6)	
		96	-0.05979(16)	0.9418(89)	-22.05(83)	6.0(1.4)	
		128	-0.05979(15)	0.9417(87)	-21.7(1.0)	5.2(1.1)	
		192	-0.05982(15)	0.9429(87)	-21.2(1.3)	3.74(51)	
	$\frac{1}{8}$	32	-0.05993(15)	0.9509(88)	-26.54(75)	3.9(1.8)	
		48	-0.05993(15)	0.9505(87)	-26.35(92)	3.9(1.8)	
		64	-0.05991(15)	0.9497(84)	-25.9(1.2)	3.9(1.8)	
		96	-0.05991(14)	0.9494(80)	-25.8(1.6)	4.0(1.8)	
		128	-0.05990(13)	0.9488(75)	-25.2(2.1)	4.1(1.8)	
		192	-0.05988(13)	0.9473(70)	-23.1(3.0)	3.1(1.4)	
	6	$\frac{1}{4}$	32	-0.05995(27)	0.962(23)	-22.34(45)	7.3(1.1)
			48	-0.05996(27)	0.962(22)	-22.41(51)	6.9(1.2)
			64	-0.05994(26)	0.960(21)	-22.36(59)	6.3(1.2)
			96	-0.05992(24)	0.957(20)	-22.19(75)	5.7(1.1)
			128	-0.05990(24)	0.954(19)	-21.85(94)	4.99(85)
			192	-0.05991(23)	0.953(18)	-21.3(1.2)	3.55(29)
$\frac{1}{8}$		48	-0.06013(23)	0.975(19)	-26.48(89)	2.22(93)	
		64	-0.06013(23)	0.975(19)	-26.5(1.0)	2.23(94)	
		96	-0.06017(23)	0.978(18)	-27.2(1.3)	2.1(1.0)	
		128	-0.06016(22)	0.978(17)	-27.1(1.8)	2.3(1.1)	
		192	-0.06011(20)	0.973(16)	-25.3(2.6)	1.72(85)	
		8	$\frac{1}{4}$	32	-0.06000(37)	0.972(40)	-22.14(49)
48				-0.06004(37)	0.977(40)	-22.29(51)	6.31(91)
64				-0.06005(37)	0.978(39)	-22.35(57)	6.08(98)
96				-0.06001(35)	0.972(37)	-22.24(70)	5.67(98)
128				-0.05996(33)	0.963(35)	-21.90(88)	5.01(77)
192				-0.05991(31)	0.954(33)	-21.3(1.2)	3.61(29)
$\frac{1}{8}$			64	-0.06030(32)	1.000(32)	-26.9(1.1)	1.68(57)
	96		-0.06035(32)	1.006(33)	-27.6(1.2)	1.42(61)	
	128		-0.06038(32)	1.009(33)	-28.0(1.5)	1.46(67)	
	192		-0.06031(30)	1.000(31)	-26.7(2.3)	1.22(58)	

TABLE S.XIV. Fits of the surface-bulk two-point function of the observable S at the ordinary UC to Eq. (17) with $\hat{\Delta} = 3$ as a function of the minimum distance z_{\min} from the surface, the maximum ratio $(z/L)_{\max}$, and the minimum lattice size L_{\min} considered in the fits. The uncertainty due to the variation of the boundary scaling dimension $\hat{\Delta}_\sigma = 2 - 0.7249(6)$ [58] within one quoted error bar largely dominates over the statistical error bars of the fits. As a reference, a fit employing only the central value of $\hat{\Delta}_\sigma$ for $z_{\min} = 4$, $(z/L)_{\max} = 1/4$, $L_{\min} = 128$ results in $M_{\phi\sigma} = 0.39501(10)$.

z_{\min}	$(z/L)_{\max}$	L_{\min}	$M_{\phi\sigma}$	z_0	$B_{\phi\sigma}$	C	$\chi^2/\text{d.o.f.}$	
4	$\frac{1}{4}$	32	0.3947(11)	1.094(11)	2.679(17)	3.022(78)	30.32(86)	
		48	0.3947(11)	1.094(11)	2.690(20)	3.017(79)	30.55(88)	
		64	0.3948(11)	1.096(11)	2.627(31)	3.037(78)	30.56(85)	
		96	0.3949(11)	1.099(11)	2.548(39)	3.058(77)	30.80(81)	
		128	0.3950(11)	1.102(11)	2.402(57)	3.086(77)	30.45(71)	
	$\frac{1}{8}$	32	0.3950(11)	1.101(11)	2.843(46)	3.086(75)	56.6(1.1)	
		48	0.3950(11)	1.102(11)	2.806(57)	3.088(75)	57.0(1.1)	
		64	0.3950(11)	1.101(11)	2.822(77)	3.085(75)	58.2(1.1)	
		96	0.3950(11)	1.101(11)	2.80(11)	3.082(75)	60.1(1.2)	
		128	0.3951(11)	1.104(11)	2.42(16)	3.108(77)	62.1(1.2)	
	$\frac{1}{10}$	48	0.3952(11)	1.107(11)	2.863(86)	3.136(74)	72.3(1.1)	
		64	0.3952(11)	1.108(11)	2.78(11)	3.138(75)	73.0(1.1)	
		96	0.3952(11)	1.107(11)	2.88(15)	3.130(75)	74.9(1.2)	
		128	0.3952(11)	1.108(11)	2.58(23)	3.138(77)	77.8(1.2)	
	6	$\frac{1}{4}$	32	0.3925(12)	1.013(14)	2.755(20)	2.14(11)	3.057(37)
48			0.3925(12)	1.011(14)	2.791(23)	2.12(11)	2.565(57)	
64			0.3925(12)	1.011(15)	2.792(29)	2.12(11)	2.241(57)	
96			0.3924(12)	1.011(14)	2.798(37)	2.12(11)	2.170(62)	
128			0.3925(12)	1.012(14)	2.770(55)	2.14(11)	2.039(42)	
$\frac{1}{8}$		48	0.3923(11)	1.007(14)	3.076(68)	2.086(99)	1.55(10)	
		64	0.3923(11)	1.007(14)	3.080(79)	2.086(99)	1.56(10)	
		96	0.3922(11)	1.005(14)	3.19(10)	2.072(99)	1.38(11)	
		128	0.3921(12)	1.003(14)	3.31(15)	2.05(10)	1.35(13)	
$\frac{1}{10}$		64	0.3922(11)	1.005(13)	3.25(13)	2.075(96)	1.73(14)	
		96	0.3922(11)	1.005(13)	3.30(15)	2.073(96)	1.73(14)	
		128	0.3921(12)	1.003(14)	3.49(22)	2.06(10)	1.64(15)	
8		$\frac{1}{4}$	32	0.3923(13)	1.002(19)	2.756(23)	2.00(18)	2.676(38)
			48	0.3922(13)	1.001(19)	2.789(25)	1.99(18)	2.240(15)
			64	0.3922(13)	0.999(20)	2.802(32)	1.96(18)	1.982(15)
	96		0.3922(13)	0.998(20)	2.817(37)	1.95(18)	1.890(11)	
	128		0.3922(13)	1.000(20)	2.799(54)	1.98(18)	1.790(19)	
	$\frac{1}{8}$	64	0.3918(12)	0.987(18)	3.152(89)	1.85(16)	0.700(12)	
		96	0.3918(12)	0.987(18)	3.22(10)	1.85(16)	0.5839(64)	
		128	0.3917(13)	0.984(19)	3.36(15)	1.81(17)	0.4473(36)	
	$\frac{1}{10}$	96	0.3916(12)	0.982(18)	3.39(17)	1.79(16)	0.526(11)	
		128	0.3916(13)	0.981(19)	3.53(23)	1.79(16)	0.438(14)	

TABLE S.XV. Fits of the two-point function of surface order parameter S at the special UC to Eq. (15), as a function of the minimum distance x_{\min} , the maximum value $(x/L)_{\max}$, and the minimum lattice size L_{\min} considered in the fits. In the quoted error bars we sum the statistical error of the fit, the variation coming from $\hat{\Delta}_\sigma$ and the variation coming from $\hat{\Delta}_\varepsilon$. As a reference, a fit employing only the central values of $\hat{\Delta}_\sigma$ and $\hat{\Delta}_\varepsilon$ for $x_{\min} = 4$, $(x/L)_{\max} = 1/4$, $L_{\min} = 48$ results in $\mathcal{N}_\sigma^2 = 0.354240(14)$.

x_{\min}	$(x/L)_{\max}$	L_{\min}	\mathcal{N}_σ^2	$B_{\sigma\sigma}$	C	$\chi^2/\text{d.o.f.}$
4	$\frac{1}{4}$	32	0.35424(56)	1.509(12)	-0.031(14)	15.0(1.4)
		48	0.35424(56)	1.509(13)	-0.031(13)	14.3(1.3)
		64	0.35424(55)	1.509(13)	-0.031(13)	13.7(1.2)
		96	0.35425(54)	1.508(14)	-0.031(13)	12.8(1.1)
		128	0.35425(54)	1.508(15)	-0.031(12)	11.71(88)
	$\frac{1}{8}$	32	0.35440(54)	1.489(15)	-0.038(12)	2.37(93)
		48	0.35441(54)	1.488(16)	-0.038(12)	2.33(96)
		64	0.35441(53)	1.488(17)	-0.038(12)	2.32(99)
		96	0.35441(52)	1.488(18)	-0.038(12)	2.27(95)
		128	0.35441(50)	1.488(20)	-0.038(11)	1.95(72)
6	$\frac{1}{4}$	32	0.35417(66)	1.5119(99)	-0.019(33)	13.73(79)
		48	0.35418(66)	1.511(10)	-0.021(32)	13.22(76)
		64	0.35419(65)	1.511(11)	-0.021(31)	12.73(73)
		96	0.35419(64)	1.510(12)	-0.021(30)	11.98(65)
		128	0.35419(63)	1.510(13)	-0.019(28)	10.97(52)
	$\frac{1}{8}$	48	0.35444(64)	1.487(12)	-0.043(29)	1.63(81)
		64	0.35445(63)	1.486(13)	-0.043(29)	1.53(79)
		96	0.35445(63)	1.486(14)	-0.044(28)	1.44(76)
		128	0.35445(61)	1.486(16)	-0.044(26)	1.35(70)
		8	$\frac{1}{4}$	32	0.35406(74)	1.5152(86)
48	0.35407(73)			1.5146(88)	0.014(60)	11.69(51)
64	0.35408(73)			1.5139(92)	0.012(59)	11.33(50)
96	0.35409(72)			1.5135(99)	0.012(57)	10.74(45)
128	0.35407(70)			1.514(11)	0.018(52)	9.68(37)
$\frac{1}{8}$	64		0.35441(71)	1.488(11)	-0.034(54)	1.08(46)
	96		0.35442(71)	1.487(11)	-0.035(54)	1.06(46)
	128		0.35442(70)	1.487(13)	-0.035(51)	1.01(44)

TABLE S.XVI. Same as Table S.XV setting $C = 0$. In the quoted error bars we sum the statistical error of the fit, the variation coming from $\hat{\Delta}_\sigma$ and the variation coming from $\hat{\Delta}_\varepsilon$. As a reference, a fit employing only the central values of $\hat{\Delta}_\sigma$ and $\hat{\Delta}_\varepsilon$ for $x_{\min} = 4$, $(x/L)_{\max} = 1/8$, $L_{\min} = 48$ results in $\mathcal{N}_\sigma^2 = 0.3538288(55)$.

x_{\min}	$(x/L)_{\max}$	L_{\min}	\mathcal{N}_σ^2	$B_{\sigma\sigma}$	$\chi^2/\text{d.o.f.}$
4	$\frac{1}{4}$	32	0.35383(38)	1.524(18)	50.3(3.8)
		48	0.35383(38)	1.524(19)	49.5(3.6)
		64	0.35383(38)	1.524(20)	49.4(3.4)
		96	0.35383(38)	1.524(21)	49.1(3.2)
		128	0.35384(38)	1.525(22)	49.2(3.0)
	$\frac{1}{8}$	32	0.35383(35)	1.524(26)	97.9(5.9)
		48	0.35383(35)	1.525(27)	96.6(5.7)
		64	0.35382(34)	1.526(28)	95.9(5.3)
		96	0.35382(34)	1.529(30)	94.1(4.9)
		128	0.35382(34)	1.532(32)	92.2(4.1)
6	$\frac{1}{4}$	32	0.35406(47)	1.515(15)	15.6(1.4)
		48	0.35406(47)	1.515(16)	15.4(1.5)
		64	0.35406(46)	1.515(16)	15.0(1.5)
		96	0.35407(46)	1.514(17)	14.2(1.4)
		128	0.35407(46)	1.514(18)	12.8(1.0)
	$\frac{1}{8}$	48	0.35414(43)	1.502(22)	16.2(3.1)
		64	0.35414(43)	1.503(22)	16.2(3.0)
		96	0.35414(42)	1.503(23)	15.7(2.8)
		128	0.35413(41)	1.505(26)	14.3(2.2)
		8	$\frac{1}{4}$	32	0.35412(53)
48	0.35412(53)			1.513(14)	12.6(1.3)
64	0.35412(52)			1.513(14)	12.0(1.2)
96	0.35413(52)			1.512(15)	11.4(1.0)
128	0.35414(51)			1.512(16)	10.49(98)
$\frac{1}{8}$	64		0.35427(49)	1.494(19)	4.1(1.8)
	96		0.35427(48)	1.495(20)	4.1(1.8)
	128		0.35427(47)	1.495(22)	3.5(1.4)

TABLE S.XVII. Fits of the energy profile at the special UC to Eq. (16), as a function of the minimum distance z_{\min} from the surface, the maximum ratio $(z/L)_{\max}$, and the minimum lattice size L_{\min} considered in the fits. We employ the fitted value of E_0 reported in Table II. In the quoted error bars we sum the statistical error of the fit, the variation coming from E_0 , the variation coming from $\hat{\Delta}$ and the variation coming from $\hat{\Delta}_\epsilon$.

z_{\min}	$(z/L)_{\max}$	L_{\min}	A_ϵ	z_0	B_ϵ	C	$\chi^2/\text{d.o.f.}$	
4	$\frac{1}{4}$	32	0.8461(33)	0.535(32)	5.556(19)	-0.09(13)	29.71	
		48	0.8457(33)	0.530(32)	5.564(20)	-0.11(13)	28.66	
		64	0.8466(33)	0.538(32)	5.548(21)	-0.09(13)	26.47	
		96	0.8486(32)	0.557(32)	5.513(23)	-0.01(13)	23.13	
		128	0.8516(31)	0.590(31)	5.460(35)	0.13(13)	19.28	
		192	0.8577(26)	0.658(27)	5.347(50)	0.43(13)	12.78	
	$\frac{1}{8}$	32	0.8393(29)	0.510(26)	5.877(25)	-0.12(10)	5.26	
		48	0.8390(30)	0.508(27)	5.885(26)	-0.12(10)	5.14	
		64	0.8389(30)	0.507(27)	5.886(29)	-0.13(10)	5.0	
		96	0.8394(31)	0.511(28)	5.873(32)	-0.12(11)	4.62	
		128	0.8396(33)	0.512(29)	5.870(38)	-0.12(11)	4.18	
		192	0.8423(34)	0.537(30)	5.801(52)	-0.03(12)	2.96	
	$\frac{1}{12}$	48	0.8379(27)	0.509(23)	5.985(30)	-0.105(86)	1.66	
		64	0.8379(28)	0.509(23)	5.986(32)	-0.105(86)	1.68	
		96	0.8381(28)	0.511(24)	5.977(35)	-0.102(88)	1.62	
		128	0.8378(31)	0.508(25)	5.987(45)	-0.115(94)	1.49	
		192	0.8392(36)	0.519(30)	5.939(64)	-0.08(11)	1.23	
		6	$\frac{1}{4}$	32	0.8475(47)	0.518(64)	5.502(30)	-0.34(37)
48	0.8464(48)			0.504(64)	5.520(31)	-0.41(37)	22.55	
64	0.8464(49)			0.502(64)	5.520(34)	-0.44(37)	21.69	
96	0.8477(50)			0.518(66)	5.499(36)	-0.37(38)	19.84	
128	0.8511(50)			0.564(68)	5.450(37)	-0.12(40)	17.14	
192	0.8602(49)			0.693(68)	5.308(48)	0.65(44)	11.82	
$\frac{1}{8}$	48		0.8404(43)	0.514(53)	5.838(38)	-0.14(30)	3.88	
	64		0.8402(43)	0.512(54)	5.844(40)	-0.14(30)	3.87	
	96		0.8402(45)	0.512(55)	5.841(43)	-0.15(30)	3.86	
	128		0.8399(49)	0.506(59)	5.848(54)	-0.19(32)	3.65	
	192		0.8428(55)	0.538(67)	5.784(70)	-0.04(37)	2.73	
	96		0.8394(41)	0.526(47)	5.945(45)	-0.02(25)	1.38	
$\frac{1}{12}$	128		0.8389(44)	0.520(49)	5.960(55)	-0.05(26)	1.34	
	192		0.8404(52)	0.534(58)	5.914(82)	0.007(303)	1.14	
	8		$\frac{1}{4}$	32	0.8479(62)	0.47(10)	5.464(40)	-1.04(75)
48				0.8473(62)	0.46(10)	5.474(41)	-1.07(75)	17.49
64				0.8464(63)	0.45(10)	5.486(44)	-1.19(74)	17.22
96				0.8469(66)	0.45(11)	5.478(48)	-1.23(76)	16.11
128		0.8494(69)		0.49(11)	5.444(54)	-1.02(82)	14.22	
192		0.8585(71)		0.64(12)	5.316(53)	0.02(93)	10.69	
$\frac{1}{8}$		64	0.8414(57)	0.512(88)	5.800(51)	-0.24(63)	2.95	
		96	0.8414(58)	0.511(89)	5.801(53)	-0.24(63)	2.98	
		128	0.8408(63)	0.500(96)	5.812(66)	-0.33(67)	2.92	
		192	0.8427(73)	0.52(11)	5.768(86)	-0.26(75)	2.36	
		96	0.8408(56)	0.543(83)	5.909(62)	0.10(58)	1.1	
		128	0.8406(58)	0.542(83)	5.918(68)	0.10(58)	1.08	
$\frac{1}{12}$		192	0.8416(65)	0.549(90)	5.886(90)	0.11(61)	0.97	

TABLE S.XVIII. Same as Table S.XVII setting $C = 0$.

z_{\min}	$(z/L)_{\max}$	L_{\min}	A_{ϵ}	z_0	B_{ϵ}	$\chi^2/\text{d.o.f.}$	
4	$\frac{1}{4}$	32	0.8475(16)	0.5535(61)	5.541(32)	29.8	
		48	0.8475(16)	0.5536(58)	5.544(36)	28.82	
		64	0.8480(15)	0.5562(56)	5.531(41)	26.54	
		96	0.8488(14)	0.5600(51)	5.510(48)	23.09	
		128	0.8494(12)	0.5636(45)	5.491(56)	19.41	
		192	0.8501(10)	0.5684(36)	5.460(66)	14.54	
	$\frac{1}{8}$	32	0.8412(15)	0.5353(53)	5.855(39)	5.7	
		48	0.8411(15)	0.5347(53)	5.861(41)	5.62	
		64	0.8412(15)	0.5351(53)	5.858(45)	5.52	
		96	0.8416(14)	0.5369(51)	5.842(50)	5.07	
		128	0.8419(13)	0.5385(48)	5.830(60)	4.57	
		192	0.8429(11)	0.5428(40)	5.790(74)	2.97	
	$\frac{1}{12}$	48	0.8397(14)	0.5319(48)	5.963(45)	2.12	
		64	0.8397(14)	0.5318(48)	5.963(48)	2.15	
		96	0.8399(14)	0.5326(49)	5.953(52)	2.07	
		128	0.8400(14)	0.5331(48)	5.950(62)	2.04	
		192	0.8410(13)	0.5367(45)	5.901(80)	1.44	
		6	$\frac{1}{4}$	32	0.8500(25)	0.566(13)	5.481(27)
48	0.8495(25)			0.563(13)	5.493(30)	22.88	
64	0.8499(24)			0.565(13)	5.487(35)	22.07	
96	0.8508(23)			0.572(12)	5.467(43)	20.07	
128	0.8522(21)			0.582(11)	5.438(53)	17.13	
192	0.8544(17)			0.5988(88)	5.382(64)	12.3	
$\frac{1}{8}$	48		0.8415(23)	0.534(11)	5.828(40)	3.97	
	64		0.8413(23)	0.533(12)	5.833(41)	3.96	
	96		0.8415(23)	0.534(12)	5.829(45)	3.95	
	128		0.8416(23)	0.535(12)	5.826(57)	3.79	
	192		0.8433(21)	0.545(11)	5.777(73)	2.74	
	96		0.8396(22)	0.528(10)	5.944(54)	1.38	
$\frac{1}{12}$	128		0.8393(23)	0.527(11)	5.956(60)	1.35	
	192		0.8403(25)	0.532(12)	5.915(81)	1.14	
	8		$\frac{1}{4}$	32	0.8524(34)	0.580(24)	5.429(29)
48				0.8520(34)	0.577(24)	5.437(29)	18.0
64				0.8519(34)	0.576(23)	5.441(31)	17.86
96				0.8529(33)	0.585(23)	5.424(38)	16.77
128		0.8548(31)		0.602(21)	5.389(50)	14.61	
192		0.8584(26)		0.635(18)	5.317(62)	10.66	
$\frac{1}{8}$		64	0.8426(31)	0.538(20)	5.791(50)	3.0	
		96	0.8425(32)	0.538(20)	5.792(52)	3.03	
		128	0.8425(33)	0.538(21)	5.796(57)	3.01	
		192	0.8442(34)	0.551(22)	5.750(72)	2.41	
		96	0.8403(30)	0.532(18)	5.914(65)	1.11	
		128	0.8400(32)	0.530(19)	5.923(72)	1.09	
$\frac{1}{12}$		192	0.8410(36)	0.536(22)	5.892(89)	0.98	

TABLE S.XIX. Fits of the S^2 profile at the special UC to Eq. (A7), as a function of the minimum distance z_{\min} from the surface, the maximum ratio $(z/L)_{\max}$, and the minimum lattice size L_{\min} considered in the fits. We employ the fitted value of S_0^2 reported in Table S.I. In the quoted error bars we sum the statistical error of the fit, the variation coming from S_0^2 , the variation coming from $\hat{\Delta}$ and the variation coming from $\hat{\Delta}_\epsilon$.

z_{\min}	$(z/L)_{\max}$	L_{\min}	A_ϵ	z_0	B_ϵ	C	$\chi^2/\text{d.o.f.}$	
4	$\frac{1}{4}$	32	0.09339(45)	0.529(38)	5.552(35)	0.04(16)	31.32	
		48	0.09334(45)	0.524(37)	5.560(36)	0.01(15)	30.23	
		64	0.09344(45)	0.532(37)	5.545(36)	0.04(15)	28.04	
		96	0.09366(44)	0.552(37)	5.510(38)	0.12(16)	24.57	
		128	0.09401(42)	0.586(36)	5.455(50)	0.27(16)	20.58	
		192	0.09471(38)	0.657(33)	5.335(66)	0.60(16)	13.68	
	$\frac{1}{8}$	32	0.09263(38)	0.505(30)	5.875(50)	0.01(12)	5.45	
		48	0.09260(39)	0.503(30)	5.883(51)	0.004(122)	5.3	
		64	0.09259(39)	0.502(31)	5.885(54)	-0.002(124)	5.17	
		96	0.09264(40)	0.505(32)	5.873(57)	0.006(129)	4.8	
		128	0.09267(42)	0.507(33)	5.869(63)	0.009(132)	4.37	
		192	0.09298(43)	0.533(34)	5.798(75)	0.11(14)	3.13	
	$\frac{1}{12}$	48	0.09249(35)	0.506(26)	5.983(59)	0.03(10)	1.62	
		64	0.09249(35)	0.505(26)	5.986(61)	0.03(10)	1.63	
		96	0.09251(36)	0.507(27)	5.977(65)	0.03(10)	1.58	
		128	0.09247(38)	0.503(29)	5.987(75)	0.02(11)	1.45	
		192	0.09263(44)	0.515(33)	5.940(94)	0.06(13)	1.19	
		6	$\frac{1}{4}$	32	0.09351(63)	0.505(73)	5.501(46)	-0.27(43)
48	0.09338(64)			0.492(73)	5.520(48)	-0.34(42)	23.83	
64	0.09337(64)			0.488(73)	5.520(50)	-0.37(42)	22.96	
96	0.09353(65)			0.504(74)	5.500(52)	-0.30(43)	21.02	
128	0.09391(66)			0.552(76)	5.449(51)	-0.04(45)	18.24	
192	0.09494(64)			0.685(78)	5.303(61)	0.76(50)	12.72	
$\frac{1}{8}$	48		0.09272(55)	0.503(60)	5.840(62)	-0.05(34)	4.0	
	64		0.09270(55)	0.502(60)	5.845(64)	-0.05(34)	3.99	
	96		0.09271(57)	0.501(62)	5.843(68)	-0.06(35)	3.98	
	128		0.09267(61)	0.495(67)	5.850(79)	-0.10(37)	3.77	
	192		0.09299(68)	0.527(74)	5.786(94)	0.05(42)	2.86	
	96		0.09263(51)	0.518(53)	5.947(74)	0.10(29)	1.34	
$\frac{1}{12}$	128		0.09257(54)	0.512(55)	5.962(85)	0.07(30)	1.3	
	192		0.09274(63)	0.525(64)	5.92(11)	0.12(34)	1.11	
	8		$\frac{1}{4}$	32	0.09352(81)	0.45(12)	5.465(56)	-1.03(86)
48				0.09345(81)	0.44(12)	5.475(57)	-1.07(86)	18.5
64				0.09335(82)	0.43(12)	5.488(60)	-1.19(85)	18.23
96				0.09340(85)	0.43(12)	5.481(65)	-1.24(87)	17.06
128		0.09369(88)		0.47(13)	5.446(69)	-1.02(92)	15.1	
192		0.09472(90)		0.62(13)	5.314(65)	0.04(1.03)	11.46	
$\frac{1}{8}$		64	0.09281(72)	0.496(99)	5.804(75)	-0.20(72)	3.04	
		96	0.09281(73)	0.50(10)	5.805(77)	-0.20(72)	3.07	
		128	0.09274(78)	0.48(11)	5.816(91)	-0.29(76)	3.0	
		192	0.09295(89)	0.50(12)	5.77(11)	-0.22(85)	2.45	
		96	0.09278(69)	0.533(91)	5.913(90)	0.19(64)	1.06	
		128	0.09275(71)	0.531(92)	5.922(96)	0.19(64)	1.04	
$\frac{1}{12}$		192	0.09286(78)	0.538(99)	5.89(12)	0.20(67)	0.94	

TABLE S.XX. Same as Table S.XIX setting $C = 0$.

z_{\min}	$(z/L)_{\max}$	L_{\min}	A_{ϵ}	z_0	B_{ϵ}	$\chi^2/\text{d.o.f.}$	
4	$\frac{1}{4}$	32	0.09333(20)	0.5220(66)	5.557(34)	31.32	
		48	0.09332(19)	0.5217(64)	5.562(38)	30.21	
		64	0.09337(18)	0.5240(60)	5.552(44)	28.03	
		96	0.09344(16)	0.5273(55)	5.535(51)	24.72	
		128	0.09350(14)	0.5307(47)	5.518(61)	21.4	
		192	0.09357(11)	0.5351(37)	5.491(73)	17.13	
	$\frac{1}{8}$	32	0.09262(18)	0.5032(59)	5.877(40)	5.49	
		48	0.09260(18)	0.5025(58)	5.884(42)	5.34	
		64	0.09260(18)	0.5026(57)	5.885(46)	5.22	
		96	0.09263(17)	0.5038(55)	5.874(52)	4.84	
		128	0.09265(16)	0.5047(51)	5.872(64)	4.41	
		192	0.09272(13)	0.5079(42)	5.845(80)	3.35	
	$\frac{1}{12}$	48	0.09243(17)	0.4991(52)	5.990(46)	1.71	
		64	0.09243(17)	0.4989(53)	5.992(49)	1.72	
		96	0.09245(17)	0.4995(53)	5.985(53)	1.68	
		128	0.09243(17)	0.4992(52)	5.994(64)	1.5	
		192	0.09249(15)	0.5012(47)	5.970(84)	1.35	
		6	$\frac{1}{4}$	32	0.09372(31)	0.543(15)	5.484(28)
48	0.09366(30)			0.540(15)	5.497(31)	24.08	
64	0.09370(29)			0.542(14)	5.493(37)	23.25	
96	0.09380(27)			0.548(13)	5.474(45)	21.19	
128	0.09395(24)			0.558(12)	5.445(56)	18.22	
192	0.09419(19)			0.5748(92)	5.389(70)	13.41	
$\frac{1}{8}$	48		0.09276(28)	0.510(13)	5.837(40)	4.05	
	64		0.09275(28)	0.509(13)	5.842(41)	4.04	
	96		0.09276(28)	0.510(13)	5.838(45)	4.03	
	128		0.09277(27)	0.511(13)	5.839(58)	3.84	
	192		0.09293(25)	0.520(11)	5.794(77)	2.9	
	96		0.09254(26)	0.504(11)	5.954(54)	1.41	
$\frac{1}{12}$	128		0.09251(27)	0.503(12)	5.968(60)	1.34	
	192		0.09261(29)	0.507(12)	5.935(83)	1.2	
	8		$\frac{1}{4}$	32	0.09402(42)	0.560(26)	5.430(29)
48				0.09397(42)	0.557(26)	5.439(30)	19.06
64				0.09395(41)	0.556(26)	5.443(31)	18.92
96				0.09406(40)	0.565(25)	5.426(39)	17.78
128		0.09428(37)		0.582(23)	5.391(52)	15.53	
192		0.09469(31)		0.615(19)	5.317(67)	11.45	
$\frac{1}{8}$		64	0.09292(38)	0.518(22)	5.797(50)	3.1	
		96	0.09291(39)	0.518(23)	5.797(52)	3.13	
		128	0.09290(40)	0.517(23)	5.802(57)	3.09	
		192	0.09309(40)	0.530(23)	5.758(74)	2.51	
		96	0.09267(36)	0.511(20)	5.921(66)	1.1	
		128	0.09264(38)	0.510(20)	5.930(73)	1.08	
$\frac{1}{12}$		192	0.09273(43)	0.515(23)	5.901(90)	0.99	

TABLE S.XXI. Fits of the surface-bulk two-point function of the observable S at the special UC to Eq. (17) as a function of the minimum distance z_{\min} from the surface, the maximum ratio $(z/L)_{\max}$, and the minimum lattice size L_{\min} considered in the fits. In the quoted error bars we sum the statistical error of the fit, the variation coming from $\hat{\Delta}_\sigma$ and the variation coming from $\hat{\Delta}_\varepsilon$.

z_{\min}	$(z/L)_{\max}$	L_{\min}	$M_{\phi\sigma}$	z_0	$B_{\phi\sigma}$	C	$\chi^2/\text{d.o.f.}$	
4	$\frac{1}{4}$	32	0.32975(53)	0.572(13)	1.2924(52)	0.650(35)	89.1(6.4)	
		48	0.32971(53)	0.570(13)	1.2934(52)	0.644(34)	87.2(6.4)	
		64	0.32976(53)	0.572(13)	1.2920(52)	0.648(34)	84.5(6.2)	
		96	0.32989(53)	0.578(13)	1.2877(56)	0.667(34)	78.3(5.8)	
		128	0.33013(52)	0.591(13)	1.2802(61)	0.708(34)	64.5(4.8)	
	$\frac{1}{8}$	32	0.32875(50)	0.543(11)	1.3635(87)	0.582(28)	10.5(1.7)	
		48	0.32872(50)	0.543(11)	1.3653(88)	0.580(28)	9.7(1.7)	
		64	0.32870(50)	0.542(11)	1.3663(89)	0.578(28)	9.6(1.8)	
		96	0.32869(50)	0.541(12)	1.3666(93)	0.577(29)	9.8(1.8)	
		128	0.32872(51)	0.543(12)	1.3651(94)	0.579(29)	9.9(1.8)	
	$\frac{1}{10}$	48	0.32866(49)	0.543(11)	1.377(10)	0.583(27)	6.4(1.1)	
		64	0.32865(49)	0.542(11)	1.377(10)	0.583(27)	6.4(1.2)	
		96	0.32863(49)	0.542(11)	1.378(11)	0.581(27)	6.5(1.2)	
		128	0.32862(50)	0.541(11)	1.379(11)	0.579(28)	6.9(1.3)	
	6	$\frac{1}{4}$	32	0.32964(61)	0.554(20)	1.2906(59)	0.554(68)	80.3(4.9)
48			0.32956(60)	0.550(20)	1.2928(60)	0.540(67)	78.9(5.0)	
64			0.32955(60)	0.549(20)	1.2928(60)	0.530(67)	77.5(4.9)	
96			0.32964(61)	0.553(20)	1.2901(61)	0.542(68)	73.0(4.7)	
128			0.32991(61)	0.570(20)	1.2833(62)	0.606(70)	61.7(4.1)	
$\frac{1}{8}$		48	0.32841(56)	0.515(17)	1.3685(95)	0.451(54)	5.32(82)	
		64	0.32840(56)	0.515(17)	1.3692(96)	0.450(54)	5.19(84)	
		96	0.32837(57)	0.513(17)	1.370(10)	0.445(55)	5.09(85)	
		128	0.32832(58)	0.510(18)	1.372(11)	0.432(58)	4.62(83)	
		64	0.32829(55)	0.514(16)	1.382(11)	0.453(50)	1.83(40)	
$\frac{1}{10}$		96	0.32828(55)	0.513(16)	1.383(11)	0.452(50)	1.80(42)	
		128	0.32824(57)	0.511(17)	1.385(12)	0.444(53)	1.67(42)	
		$\frac{1}{4}$	32	0.32967(67)	0.546(28)	1.2868(66)	0.48(12)	71.5(3.9)
			48	0.32963(67)	0.545(28)	1.2882(66)	0.48(12)	70.2(4.0)
64			0.32957(67)	0.540(28)	1.2894(66)	0.45(12)	69.8(4.0)	
96	0.32959(68)		0.538(28)	1.2885(69)	0.43(12)	67.2(3.9)		
128	0.32978(69)		0.551(29)	1.2838(70)	0.47(13)	58.1(3.5)		
$\frac{1}{8}$	64	0.32832(63)	0.502(24)	1.368(10)	0.367(96)	4.08(53)		
	96	0.32830(63)	0.502(24)	1.368(10)	0.368(96)	4.01(54)		
	128	0.32822(65)	0.496(25)	1.371(11)	0.34(10)	3.59(53)		
	$\frac{1}{10}$	96	0.32818(62)	0.501(23)	1.382(12)	0.375(91)	1.21(22)	
		128	0.32815(63)	0.499(24)	1.384(13)	0.370(92)	1.11(23)	

TABLE S.XXII. Fit of E_{surf} at the special UC to Eq. (19), as a function of the minimum lattice size L_{\min} taken into account. The quoted error bars are the sum of the statistical uncertainty obtained from the fit procedure and the variation of the fitted parameters on varying the surface exponent $\hat{\Delta}_\varepsilon = 2 - 0.718(6)$ [68] within one error bar.

L_{\min}	\mathcal{E}_0	$U_\mathcal{E}$	$\chi^2/\text{d.o.f.}$
32	1.322907(11)	2.121(19)	0.46(10)
48	1.322908(10)	2.120(22)	0.507(78)
64	1.322912(10)	2.116(22)	0.178(57)

TABLE S.XXIII. Same as Table S.XXII for the fits of S_{surf}^2 at the special UC to Eq. (A8).

L_{\min}	Σ_0	U_{σ^2}	$\chi^2/\text{d.o.f.}$
32	0.6694465(12)	0.2310(21)	0.493(32)
48	0.6694466(11)	0.2310(23)	0.584(44)
64	0.6694469(11)	0.2306(25)	0.381(79)

TABLE S.XXIV. Fits of the two-point function of energy observable on the surface at the special UC to Eq. (20), as a function of the minimum distance x_{\min} , the maximum value $(x/L)_{\max}$, and the minimum lattice size L_{\min} considered in the fits. The variation of the boundary scaling dimension $\hat{\Delta}_\varepsilon = 2 - 0.718(2)$ [68] within one quoted error bar gives the leading contribution to the total uncertainty.

x_{\min}	$(x/L)_{\max}$	L_{\min}	$\mathcal{N}_\varepsilon^2$	$B_{\varepsilon\varepsilon}$	C	$\chi^2/\text{d.o.f.}$
4	$\frac{1}{4}$	32	1.481(14)	1.803(17)	0.828(63)	4.36(93)
		48	1.481(14)	1.805(21)	0.829(62)	4.16(87)
		64	1.480(13)	1.815(29)	0.829(61)	3.55(98)
		96	1.480(13)	1.824(42)	0.829(60)	3.1(1.0)
		128	1.480(13)	1.826(61)	0.828(58)	2.50(90)
	$\frac{1}{8}$	32	1.480(14)	1.824(18)	0.830(63)	5.8(2.0)
		48	1.480(14)	1.824(20)	0.830(62)	5.8(2.0)
		64	1.480(13)	1.831(27)	0.831(62)	4.9(1.8)
		96	1.480(13)	1.840(39)	0.831(60)	4.2(2.0)
		128	1.480(13)	1.840(59)	0.830(58)	3.6(1.8)
6	$\frac{1}{4}$	32	1.482(16)	1.774(12)	0.80(15)	1.76(24)
		48	1.482(16)	1.771(15)	0.80(14)	1.69(26)
		64	1.482(16)	1.780(20)	0.81(14)	1.44(20)
		96	1.482(16)	1.788(30)	0.81(14)	1.41(23)
		128	1.482(16)	1.792(43)	0.81(13)	1.28(22)
	$\frac{1}{8}$	48	1.482(16)	1.789(16)	0.80(14)	1.94(55)
		64	1.481(16)	1.795(18)	0.81(14)	1.74(52)
		96	1.481(16)	1.806(26)	0.81(14)	1.43(42)
		128	1.481(16)	1.809(39)	0.81(14)	1.38(39)
		8	$\frac{1}{4}$	32	1.483(18)	1.767(12)
48	1.483(18)			1.761(13)	0.76(27)	1.141(85)
64	1.483(18)			1.762(18)	0.76(27)	1.044(84)
96	1.483(18)			1.766(25)	0.77(26)	1.053(92)
128	1.483(18)			1.770(36)	0.77(26)	1.010(95)
$\frac{1}{8}$	64		1.482(18)	1.779(19)	0.77(26)	0.99(13)
	96		1.482(18)	1.787(22)	0.78(26)	0.91(13)
	128		1.482(18)	1.788(31)	0.78(26)	0.94(14)

TABLE S.XXV. Fits of the two-point function of S^2 on the surface at the special UC to Eq. (A11), as a function of the minimum distance x_{\min} , the maximum value $(x/L)_{\max}$, and the minimum lattice size L_{\min} considered in the fits. The variation of the boundary scaling dimension $\hat{\Delta}_\varepsilon = 2 - 0.718(2)$ [68] within one quoted error bar gives the leading contribution to the total uncertainty.

x_{\min}	$(x/L)_{\max}$	L_{\min}	$\mathcal{N}_{\sigma^2}^2$	$B_{\varepsilon\varepsilon}$	C	$\chi^2/\text{d.o.f.}$
4	$\frac{1}{4}$	32	0.01760(16)	1.756(16)	0.270(60)	3.9(1.4)
		48	0.01760(16)	1.764(22)	0.271(60)	3.3(1.3)
		64	0.01760(16)	1.776(29)	0.273(59)	2.5(1.0)
		96	0.01760(16)	1.785(41)	0.273(57)	2.4(1.2)
		128	0.01760(15)	1.790(59)	0.273(55)	2.2(1.1)
	$\frac{1}{8}$	32	0.01760(16)	1.767(18)	0.271(60)	5.7(2.9)
		48	0.01760(16)	1.773(20)	0.272(60)	5.1(2.7)
		64	0.01760(16)	1.784(27)	0.273(59)	3.9(2.3)
		96	0.01759(16)	1.795(38)	0.275(58)	3.3(2.2)
		128	0.01759(15)	1.799(57)	0.274(56)	3.1(2.1)
6	$\frac{1}{4}$	32	0.01761(19)	1.750(11)	0.25(14)	1.92(32)
		48	0.01761(19)	1.750(15)	0.25(14)	1.77(32)
		64	0.01761(19)	1.760(20)	0.26(14)	1.36(25)
		96	0.01760(19)	1.768(29)	0.26(14)	1.32(28)
		128	0.01760(19)	1.775(40)	0.26(13)	1.24(28)
	$\frac{1}{8}$	48	0.01761(19)	1.762(16)	0.25(14)	2.07(67)
		64	0.01760(19)	1.770(18)	0.26(14)	1.71(62)
		96	0.01760(19)	1.782(25)	0.27(14)	1.30(50)
		128	0.01760(19)	1.787(36)	0.27(13)	1.26(48)
		8	$\frac{1}{4}$	32	0.01761(22)	1.753(11)
48	0.01762(22)			1.748(13)	0.22(27)	1.23(12)
64	0.01762(22)			1.749(17)	0.23(26)	1.06(12)
96	0.01761(22)			1.753(23)	0.24(26)	1.05(13)
128	0.01761(21)			1.760(32)	0.24(25)	1.02(14)
$\frac{1}{8}$	64		0.01761(22)	1.762(17)	0.23(26)	0.96(16)
	96		0.01761(22)	1.770(20)	0.24(26)	0.86(18)
	128		0.01761(22)	1.774(28)	0.25(26)	0.89(19)

TABLE S.XXVI. Fits of the energy profile at the normal UC realized with $(+, o)$ to Eq. (16), as a function of the minimum distance z_{\min} from the surface, the maximum ratio $(z/L)_{\max}$, and the minimum lattice size L_{\min} considered in the fits. We employ the fitted value of E_0 reported in Table II. Varying E_0 and Δ_ϵ within one error bar quoted in Table II results in a significant additional uncertainty in the results. As a reference, a fit employing only the central values of E_0 and of Δ_ϵ for $z_{\min} = 8$, $(z/L)_{\max} = 1/4$, $L_{\min} = 96$ results in $A_\epsilon = 4.8273(19)$.

z_{\min}	$(z/L)_{\max}$	L_{\min}	A_ϵ	z_0	B_ϵ	C	$\chi^2/\text{d.o.f.}$
4	$\frac{1}{4}$	32	4.8317(39)	1.4260(73)	-2.660(35)	-0.311(34)	4.04
		48	4.8326(39)	1.4280(72)	-2.702(42)	-0.302(33)	3.2
		64	4.8331(38)	1.4292(71)	-2.729(49)	-0.296(32)	2.93
		96	4.8339(37)	1.4311(68)	-2.773(61)	-0.287(31)	2.48
		128	4.8346(35)	1.4327(64)	-2.822(75)	-0.278(29)	2.06
		192	4.8349(34)	1.4336(60)	-2.86(10)	-0.274(27)	1.96
	$\frac{1}{8}$	32	4.8346(34)	1.4332(59)	-2.659(65)	-0.274(26)	1.15
		48	4.8347(34)	1.4334(59)	-2.682(78)	-0.274(26)	1.12
		64	4.8348(34)	1.4336(59)	-2.698(99)	-0.273(26)	1.12
		96	4.8352(33)	1.4343(59)	-2.76(13)	-0.270(26)	1.06
		128	4.8357(33)	1.4354(57)	-2.85(16)	-0.265(25)	1.0
		192	4.8361(31)	1.4362(54)	-2.94(22)	-0.261(24)	1.01
6	$\frac{1}{4}$	32	4.8276(54)	1.409(14)	-2.651(32)	-0.451(86)	3.09
		48	4.8287(54)	1.412(14)	-2.688(38)	-0.431(86)	2.37
		64	4.8293(54)	1.414(14)	-2.709(43)	-0.418(85)	2.2
		96	4.8305(53)	1.418(13)	-2.746(53)	-0.395(84)	1.93
		128	4.8316(51)	1.421(13)	-2.791(66)	-0.371(80)	1.66
		192	4.8323(48)	1.423(12)	-2.827(91)	-0.357(73)	1.64
	$\frac{1}{8}$	48	4.8325(46)	1.425(11)	-2.676(78)	-0.341(66)	0.72
		64	4.8326(47)	1.425(11)	-2.679(90)	-0.341(66)	0.72
		96	4.8329(47)	1.426(11)	-2.73(11)	-0.336(67)	0.69
		128	4.8334(48)	1.427(11)	-2.78(14)	-0.329(68)	0.67
		192	4.8336(48)	1.428(11)	-2.82(20)	-0.325(68)	0.72
		8	$\frac{1}{4}$	32	4.8245(69)	1.392(22)	-2.661(33)
48	4.8253(70)			1.394(22)	-2.683(36)	-0.62(18)	1.93
64	4.8260(70)			1.397(22)	-2.700(40)	-0.60(18)	1.79
96	4.8273(70)			1.402(22)	-2.732(48)	-0.56(18)	1.61
128	4.8288(69)			1.407(22)	-2.771(59)	-0.52(18)	1.43
192	4.8296(65)			1.410(21)	-2.801(84)	-0.49(17)	1.47
$\frac{1}{8}$	64		4.8311(60)	1.418(18)	-2.689(91)	-0.41(14)	0.62
	96		4.8313(61)	1.418(18)	-2.72(11)	-0.41(14)	0.59
	128		4.8318(62)	1.420(18)	-2.76(13)	-0.40(14)	0.59
	192		4.8317(66)	1.419(20)	-2.77(19)	-0.40(15)	0.62

TABLE S.XXVII. Same as Table S.XXVI for the normal UC realized with (+, +) BCs. Varying E_0 and Δ_ϵ within one error bar quoted in Table II results in a significant additional uncertainty in the results. As a reference, a fit employing only the central values of E_0 and of Δ_ϵ for $z_{\min} = 6$, $(z/L)_{\max} = 1/4$, $L_{\min} = 128$ results in $A_\epsilon = 4.8364(14)$.

z_{\min}	$(z/L)_{\max}$	L_{\min}	A_ϵ	z_0	B_ϵ	C	$\chi^2/\text{d.o.f.}$
4	$\frac{1}{4}$	32	4.8397(38)	1.4448(73)	3.591(29)	-0.217(35)	4.92
		48	4.8386(37)	1.4426(71)	3.651(36)	-0.227(34)	3.04
		64	4.8379(36)	1.4409(68)	3.692(44)	-0.236(32)	2.37
		96	4.8370(34)	1.4388(64)	3.747(57)	-0.246(30)	1.51
		128	4.8368(33)	1.4383(61)	3.763(74)	-0.249(28)	1.45
		192	4.8368(31)	1.4380(57)	3.78(10)	-0.251(26)	1.45
	$\frac{1}{8}$	32	4.8387(32)	1.4420(57)	3.425(61)	-0.233(26)	1.63
		48	4.8385(32)	1.4416(57)	3.477(76)	-0.235(26)	1.45
		64	4.8383(32)	1.4412(56)	3.511(93)	-0.236(26)	1.42
		96	4.8380(32)	1.4406(56)	3.57(13)	-0.238(26)	1.36
		128	4.8381(31)	1.4408(56)	3.55(16)	-0.238(25)	1.44
		192	4.8382(30)	1.4411(52)	3.53(22)	-0.236(24)	1.62
6	$\frac{1}{4}$	32	4.8407(55)	1.449(15)	3.597(23)	-0.176(95)	4.36
		48	4.8396(55)	1.447(14)	3.647(28)	-0.193(94)	2.91
		64	4.8385(53)	1.443(14)	3.689(35)	-0.214(91)	2.28
		96	4.8369(51)	1.438(13)	3.749(45)	-0.248(86)	1.47
		128	4.8364(49)	1.437(13)	3.769(61)	-0.260(81)	1.39
		192	4.8361(46)	1.436(12)	3.788(87)	-0.270(75)	1.34
	$\frac{1}{8}$	48	4.8384(45)	1.442(11)	3.507(71)	-0.232(68)	1.32
		64	4.8383(45)	1.441(11)	3.525(81)	-0.234(67)	1.31
		96	4.8380(45)	1.441(11)	3.57(11)	-0.238(68)	1.29
		128	4.8381(46)	1.441(11)	3.56(14)	-0.237(69)	1.37
		192	4.8383(46)	1.442(11)	3.53(19)	-0.231(70)	1.51
		8	$\frac{1}{4}$	32	4.8413(73)	1.455(24)	3.622(19)
48	4.8407(72)			1.453(24)	3.646(22)	-0.12(20)	2.73
64	4.8396(71)			1.449(24)	3.684(28)	-0.15(20)	2.19
96	4.8374(69)			1.441(23)	3.745(37)	-0.22(19)	1.41
128	4.8366(67)			1.438(22)	3.768(52)	-0.25(18)	1.33
192	4.8357(63)			1.434(20)	3.794(78)	-0.29(17)	1.27
$\frac{1}{8}$	64		4.8386(59)	1.443(18)	3.539(81)	-0.21(14)	1.24
	96		4.8384(59)	1.443(18)	3.57(10)	-0.22(14)	1.22
	128		4.8385(61)	1.443(18)	3.56(13)	-0.21(14)	1.27
	192		4.8387(64)	1.444(19)	3.53(18)	-0.21(15)	1.39

TABLE S.XXVIII. Fits of the S^2 profile at the normal UC realized with (+, o) BCs to Eq. (A7), as a function of the minimum distance z_{\min} from the surface, the maximum ratio $(z/L)_{\max}$, and the minimum lattice size L_{\min} considered in the fits. We employ the fitted value of S_0^2 reported in Table S.I. Varying S_0^2 and Δ_ϵ within one error bar quoted in Table S.I results in a significant additional uncertainty in the results. As a reference, a fit employing only the central values of S_0^2 and of Δ_ϵ for $z_{\min} = 4$, $(z/L)_{\max} = 1/8$, $L_{\min} = 192$ results in $A_{S^2} = 0.53396(12)$.

z_{\min}	$(z/L)_{\max}$	L_{\min}	A_{S^2}	z_0	\mathcal{B}_ϵ	C	$\chi^2/\text{d.o.f.}$
4	$\frac{1}{4}$	32	0.53347(49)	1.4217(83)	-2.677(38)	-0.226(39)	4.32
		48	0.53356(49)	1.4235(82)	-2.716(46)	-0.217(38)	3.54
		64	0.53362(47)	1.4246(80)	-2.741(54)	-0.212(37)	3.29
		96	0.53370(46)	1.4264(77)	-2.784(67)	-0.202(35)	2.86
		128	0.53378(44)	1.4281(72)	-2.835(83)	-0.194(33)	2.39
		192	0.53383(42)	1.4291(67)	-2.88(11)	-0.189(31)	2.25
	$\frac{1}{8}$	32	0.53381(42)	1.4289(66)	-2.689(67)	-0.188(29)	1.16
		48	0.53381(42)	1.4291(66)	-2.707(82)	-0.188(29)	1.14
		64	0.53382(42)	1.4292(66)	-2.72(10)	-0.187(30)	1.15
		96	0.53386(41)	1.4299(66)	-2.78(13)	-0.184(29)	1.11
		128	0.53391(40)	1.4309(63)	-2.87(17)	-0.179(28)	1.05
		192	0.53396(38)	1.4317(60)	-2.95(24)	-0.176(26)	1.07
6	$\frac{1}{4}$	32	0.53302(68)	1.405(15)	-2.667(35)	-0.366(98)	3.33
		48	0.53314(68)	1.408(15)	-2.701(41)	-0.347(98)	2.67
		64	0.53320(67)	1.410(15)	-2.721(47)	-0.335(97)	2.51
		96	0.53332(66)	1.413(15)	-2.757(58)	-0.312(95)	2.26
		128	0.53345(63)	1.416(14)	-2.803(72)	-0.288(90)	1.96
		192	0.53353(59)	1.419(13)	-2.84(10)	-0.272(82)	1.91
	$\frac{1}{8}$	48	0.53358(57)	1.421(12)	-2.697(80)	-0.253(74)	0.76
		64	0.53358(58)	1.421(12)	-2.699(93)	-0.253(74)	0.77
		96	0.53361(58)	1.422(12)	-2.74(12)	-0.249(75)	0.74
		128	0.53367(59)	1.423(12)	-2.80(14)	-0.241(76)	0.73
		192	0.53369(58)	1.424(12)	-2.84(21)	-0.237(75)	0.78
		8	$\frac{1}{4}$	32	0.53265(87)	1.386(25)	-2.674(36)
48	0.53274(87)			1.389(25)	-2.695(39)	-0.55(20)	2.15
64	0.53281(87)			1.391(25)	-2.712(43)	-0.53(20)	2.02
96	0.53295(87)			1.396(25)	-2.742(52)	-0.49(20)	1.86
128	0.53311(85)			1.401(24)	-2.782(64)	-0.44(20)	1.67
192	0.53322(81)			1.405(23)	-2.816(91)	-0.41(18)	1.69
$\frac{1}{8}$	64		0.53340(74)	1.413(20)	-2.707(94)	-0.33(15)	0.64
	96		0.53342(75)	1.414(20)	-2.73(11)	-0.33(15)	0.61
	128		0.53347(76)	1.415(20)	-2.78(13)	-0.32(16)	0.61
	192		0.53347(80)	1.415(21)	-2.78(20)	-0.32(16)	0.64

TABLE S.XXIX. Same as Table S.XXVIII for the normal UC realized with (+, +) BCs. Varying S_0^2 within one error bar quoted in Table S.I results in a significant additional uncertainty in the results. As a reference, a fit employing only the central values of S_0^2 and of Δ_ϵ for $z_{\min} = 6$, $(z/L)_{\max} = 1/4$, $L_{\min} = 128$ results in $A_{S^2} = 0.53398(15)$.

z_{\min}	$(z/L)_{\max}$	L_{\min}	A_{S^2}	z_0	B_ϵ	C	$\chi^2/\text{d.o.f.}$	
4	$\frac{1}{4}$	32	0.53431(48)	1.4395(83)	3.603(32)	-0.135(39)	4.47	
		48	0.53421(47)	1.4375(81)	3.658(40)	-0.145(38)	2.84	
		64	0.53414(45)	1.4360(77)	3.696(49)	-0.153(37)	2.26	
		96	0.53405(43)	1.4340(73)	3.746(63)	-0.162(34)	1.5	
		128	0.53403(41)	1.4337(69)	3.757(83)	-0.165(32)	1.52	
		192	0.53403(39)	1.4336(64)	3.77(11)	-0.165(30)	1.54	
	$\frac{1}{8}$	32	0.53422(40)	1.4371(64)	3.460(62)	-0.149(29)	1.56	
		48	0.53420(40)	1.4367(64)	3.507(79)	-0.151(29)	1.4	
		64	0.53419(39)	1.4364(63)	3.536(97)	-0.152(29)	1.4	
		96	0.53416(39)	1.4359(63)	3.59(13)	-0.154(29)	1.36	
		128	0.53417(39)	1.4362(62)	3.56(17)	-0.153(28)	1.44	
		192	0.53419(37)	1.4365(58)	3.53(23)	-0.151(26)	1.61	
	6	$\frac{1}{4}$	32	0.53440(69)	1.443(16)	3.610(24)	-0.10(11)	4.01
			48	0.53429(68)	1.441(16)	3.655(30)	-0.12(11)	2.72
64			0.53418(66)	1.438(16)	3.693(37)	-0.14(10)	2.19	
96			0.53402(64)	1.433(15)	3.748(49)	-0.169(97)	1.45	
128			0.53398(61)	1.432(14)	3.763(67)	-0.178(91)	1.44	
192			0.53396(57)	1.431(13)	3.776(96)	-0.185(83)	1.44	
$\frac{1}{8}$		48	0.53419(56)	1.437(12)	3.531(72)	-0.149(75)	1.31	
		64	0.53418(56)	1.437(12)	3.546(83)	-0.150(75)	1.3	
		96	0.53416(56)	1.436(12)	3.58(11)	-0.154(76)	1.29	
		128	0.53417(57)	1.436(12)	3.57(14)	-0.152(76)	1.37	
8	$\frac{1}{4}$	192	0.53420(57)	1.437(12)	3.53(20)	-0.146(77)	1.52	
		32	0.53444(91)	1.447(27)	3.634(19)	-0.06(22)	3.16	
		48	0.53438(90)	1.445(27)	3.656(23)	-0.07(22)	2.58	
		64	0.53426(89)	1.442(26)	3.690(29)	-0.09(22)	2.11	
		96	0.53405(86)	1.434(26)	3.747(39)	-0.16(21)	1.42	
		128	0.53397(83)	1.432(24)	3.764(56)	-0.18(20)	1.39	
		192	0.53390(78)	1.428(23)	3.783(85)	-0.21(18)	1.35	
		$\frac{1}{8}$	64	0.53421(73)	1.438(20)	3.557(81)	-0.14(16)	1.23
			96	0.53419(73)	1.438(20)	3.58(10)	-0.14(16)	1.21
			128	0.53420(74)	1.438(20)	3.57(13)	-0.14(16)	1.27
	192		0.53424(77)	1.439(21)	3.54(18)	-0.13(17)	1.39	

TABLE S.XXX. Fits of the profile of the order-parameter S at the normal UC realized with (+, o) to Eq. (21), as a function of the minimum distance z_{\min} from the surface, the maximum ratio $(z/L)_{\max}$, and the minimum lattice size L_{\min} considered in the fits. A variation of the critical exponent $\Delta_\phi = 0.518\,148\,9(10)$ [66] within one error bar gives a negligible increase in the uncertainty of the fitted parameters.

z_{\min}	$(z/L)_{\max}$	L_{\min}	A_ϕ	z_0	B_ϕ	C	$\chi^2/\text{d.o.f.}$
4	$\frac{1}{4}$	32	1.126327(63)	1.4363(15)	-1.0123(39)	-0.0870(27)	2.77
		48	1.126369(64)	1.4375(15)	-1.0190(45)	-0.0848(28)	1.91
		64	1.126399(64)	1.4383(15)	-1.0241(50)	-0.0832(28)	1.52
		96	1.126440(65)	1.4395(15)	-1.0313(56)	-0.0809(28)	0.98
		128	1.126469(63)	1.4404(15)	-1.0378(59)	-0.0791(27)	0.55
		192	1.126478(63)	1.4407(15)	-1.0412(71)	-0.0786(26)	0.48
	$\frac{1}{8}$	32	1.126439(62)	1.4399(14)	-0.995(12)	-0.0798(24)	0.61
		48	1.126445(64)	1.4400(14)	-0.999(14)	-0.0796(25)	0.58
		64	1.126450(66)	1.4401(15)	-1.003(17)	-0.0795(26)	0.55
		96	1.126465(69)	1.4405(16)	-1.013(21)	-0.0788(27)	0.51
		128	1.126486(70)	1.4410(16)	-1.027(23)	-0.0779(28)	0.45
		192	1.126499(73)	1.4413(17)	-1.038(28)	-0.0773(29)	0.44
6	$\frac{1}{4}$	32	1.126195(84)	1.4293(27)	-1.0108(40)	-0.1098(69)	2.13
		48	1.126245(86)	1.4310(28)	-1.0166(46)	-0.1056(71)	1.43
		64	1.126283(88)	1.4324(29)	-1.0210(51)	-0.1020(73)	1.14
		96	1.126341(91)	1.4346(30)	-1.0278(58)	-0.0963(75)	0.74
		128	1.126391(90)	1.4366(29)	-1.0344(62)	-0.0910(74)	0.4
		192	1.126409(89)	1.4373(29)	-1.0375(75)	-0.0890(73)	0.36
	$\frac{1}{8}$	48	1.126377(89)	1.4367(27)	-1.000(16)	-0.0897(63)	0.35
		64	1.126377(91)	1.4367(27)	-1.000(18)	-0.0896(64)	0.36
		96	1.126391(97)	1.4371(29)	-1.007(22)	-0.0888(68)	0.33
		128	1.12641(10)	1.4378(31)	-1.018(26)	-0.0872(73)	0.3
		192	1.12642(11)	1.4380(35)	-1.022(34)	-0.0869(83)	0.31
		8	$\frac{1}{4}$	32	1.12611(11)	1.4229(46)	-1.0125(42)
48	1.12614(11)			1.4242(46)	-1.0157(46)	-0.134(15)	1.19
64	1.12619(11)			1.4262(48)	-1.0198(52)	-0.128(15)	0.94
96	1.12626(12)			1.4294(51)	-1.0261(60)	-0.117(16)	0.62
128	1.12633(12)			1.4328(52)	-1.0326(65)	-0.106(17)	0.33
192	1.12636(13)			1.4341(54)	-1.0353(82)	-0.102(18)	0.32
$\frac{1}{8}$	64		1.12634(12)	1.4345(46)	-1.003(20)	-0.099(14)	0.32
	96		1.12635(12)	1.4347(47)	-1.007(22)	-0.098(14)	0.3
	128		1.12637(13)	1.4355(50)	-1.016(27)	-0.096(15)	0.27
	192		1.12637(16)	1.4356(61)	-1.017(38)	-0.096(18)	0.28

TABLE S.XXXI. Same as Table S.XXX for the normal UC realized with (+, +) BCs.

z_{\min}	$(z/L)_{\max}$	L_{\min}	A_{ϕ}	z_0	B_{ϕ}	C	$\chi^2/\text{d.o.f.}$	
4	$\frac{1}{4}$	32	1.126914(62)	1.4536(16)	1.3235(33)	-0.0535(30)	16.57	
		48	1.126823(61)	1.4512(16)	1.3415(37)	-0.0578(29)	9.56	
		64	1.126755(60)	1.4492(15)	1.3546(40)	-0.0616(29)	6.62	
		96	1.126672(60)	1.4468(15)	1.3714(43)	-0.0663(28)	3.28	
		128	1.126632(59)	1.4456(15)	1.3817(53)	-0.0688(28)	2.34	
		192	1.126607(58)	1.4447(15)	1.3908(62)	-0.0704(27)	1.61	
	$\frac{1}{8}$	32	1.126733(56)	1.4476(13)	1.285(12)	-0.0657(25)	2.77	
		48	1.126711(57)	1.4472(14)	1.304(14)	-0.0664(25)	2.22	
		64	1.126690(57)	1.4467(14)	1.319(16)	-0.0671(25)	2.02	
		96	1.126664(60)	1.4461(14)	1.338(20)	-0.0682(26)	1.83	
		128	1.126663(63)	1.4460(15)	1.339(23)	-0.0683(27)	1.95	
		192	1.126647(65)	1.4456(16)	1.353(27)	-0.0690(29)	2.11	
	6	$\frac{1}{4}$	32	1.127119(90)	1.4645(32)	1.3191(35)	-0.0181(83)	14.67
			48	1.127024(90)	1.4616(32)	1.3348(39)	-0.0245(82)	8.58
64			1.126931(89)	1.4582(31)	1.3479(42)	-0.0329(82)	5.9	
96			1.126798(89)	1.4531(31)	1.3658(46)	-0.0462(82)	2.88	
128			1.126726(89)	1.4502(31)	1.3769(56)	-0.0542(81)	2.09	
192			1.126668(89)	1.4478(31)	1.3872(65)	-0.0610(81)	1.44	
$\frac{1}{8}$		48	1.126789(84)	1.4511(28)	1.306(15)	-0.0542(69)	1.77	
		64	1.126776(85)	1.4508(28)	1.314(17)	-0.0547(70)	1.65	
		96	1.126751(89)	1.4500(29)	1.329(21)	-0.0562(72)	1.51	
		128	1.126755(96)	1.4502(31)	1.327(25)	-0.0559(76)	1.61	
		192	1.12674(11)	1.4497(35)	1.335(32)	-0.0571(88)	1.75	
		8	$\frac{1}{4}$	32	1.12727(12)	1.4758(53)	1.3218(41)	0.031(17)
48				1.12722(12)	1.4744(53)	1.3302(42)	0.029(17)	7.73
64				1.12712(12)	1.4705(53)	1.3423(46)	0.018(17)	5.23
96	1.12695(12)			1.4629(54)	1.3605(51)	-0.007(18)	2.44	
128	1.12685(12)			1.4576(55)	1.3719(63)	-0.024(18)	1.79	
192	1.12674(13)			1.4524(56)	1.3835(74)	-0.043(18)	1.23	
$\frac{1}{8}$	64		1.12686(12)	1.4557(49)	1.315(19)	-0.035(15)	1.28	
	96		1.12684(12)	1.4554(49)	1.323(21)	-0.036(15)	1.19	
	128		1.12685(13)	1.4555(52)	1.321(26)	-0.036(16)	1.25	
	192		1.12683(15)	1.4549(63)	1.326(36)	-0.038(19)	1.37	

TABLE S.XXXII. Same as Table S.XXXI, fixing $C = 0$.

z_{\min}	$(z/L)_{\max}$	L_{\min}	A_{ϕ}	z_0	B_{ϕ}	$\chi^2/\text{d.o.f.}$	
4	$\frac{1}{4}$	32	1.127577(29)	1.47748(28)	1.2932(36)	32.31	
		48	1.127548(29)	1.47711(28)	1.3056(39)	28.09	
		64	1.127534(28)	1.47694(27)	1.3121(43)	27.79	
		96	1.127522(28)	1.47677(26)	1.3189(47)	28.12	
		128	1.127517(28)	1.47672(26)	1.3201(57)	30.08	
		192	1.127510(28)	1.47665(26)	1.3215(67)	33.11	
	$\frac{1}{8}$	32	1.127647(27)	1.47810(25)	1.163(12)	44.98	
		48	1.127645(27)	1.47807(25)	1.166(13)	45.33	
		64	1.127655(26)	1.47818(24)	1.150(15)	45.91	
		96	1.127674(27)	1.47838(24)	1.120(18)	46.49	
		128	1.127704(27)	1.47874(25)	1.060(20)	45.79	
		192	1.127723(27)	1.47898(24)	0.998(23)	46.37	
	6	$\frac{1}{4}$	32	1.127242(40)	1.47041(54)	1.3145(34)	14.89
			48	1.127193(40)	1.46959(54)	1.3282(37)	9.07
64			1.127159(39)	1.46903(53)	1.3382(40)	6.82	
96			1.127126(38)	1.46845(52)	1.3498(45)	4.72	
128			1.127115(38)	1.46827(51)	1.3550(54)	4.66	
192			1.127108(38)	1.46814(50)	1.3593(64)	4.85	
$\frac{1}{8}$		48	1.127218(37)	1.46971(48)	1.260(14)	6.1	
		64	1.127212(37)	1.46962(48)	1.266(15)	6.1	
		96	1.127208(38)	1.46956(50)	1.269(19)	6.23	
		128	1.127227(39)	1.46985(51)	1.247(21)	6.19	
		192	1.127244(39)	1.47012(50)	1.222(24)	6.29	
		8	$\frac{1}{4}$	32	1.127132(52)	1.46772(91)	1.3264(34)
48				1.127093(52)	1.46694(91)	1.3344(36)	7.87
64				1.127043(51)	1.46589(90)	1.3451(39)	5.28
96	1.126983(50)			1.46461(88)	1.3593(43)	2.44	
128	1.126960(50)			1.46411(87)	1.3666(53)	1.91	
192	1.126947(49)			1.46379(86)	1.3727(62)	1.61	
$\frac{1}{8}$	64		1.127042(49)	1.46546(82)	1.300(17)	1.69	
	96		1.127033(51)	1.46529(85)	1.307(19)	1.63	
	128		1.127042(54)	1.46545(89)	1.300(22)	1.68	
	192		1.127050(55)	1.46561(93)	1.293(26)	1.83	